USGS
science for a changing world

Prepared in cooperation with the Chicago District of the U.S. Army Corps of Engineers

Comparison of Index Velocity Measurements Made With a Horizontal Acoustic Doppler Current Profiler and a Three-Path Acoustic Velocity Meter for Computation of Discharge in the Chicago Sanitary and Ship Canal near Lemont, Illinois

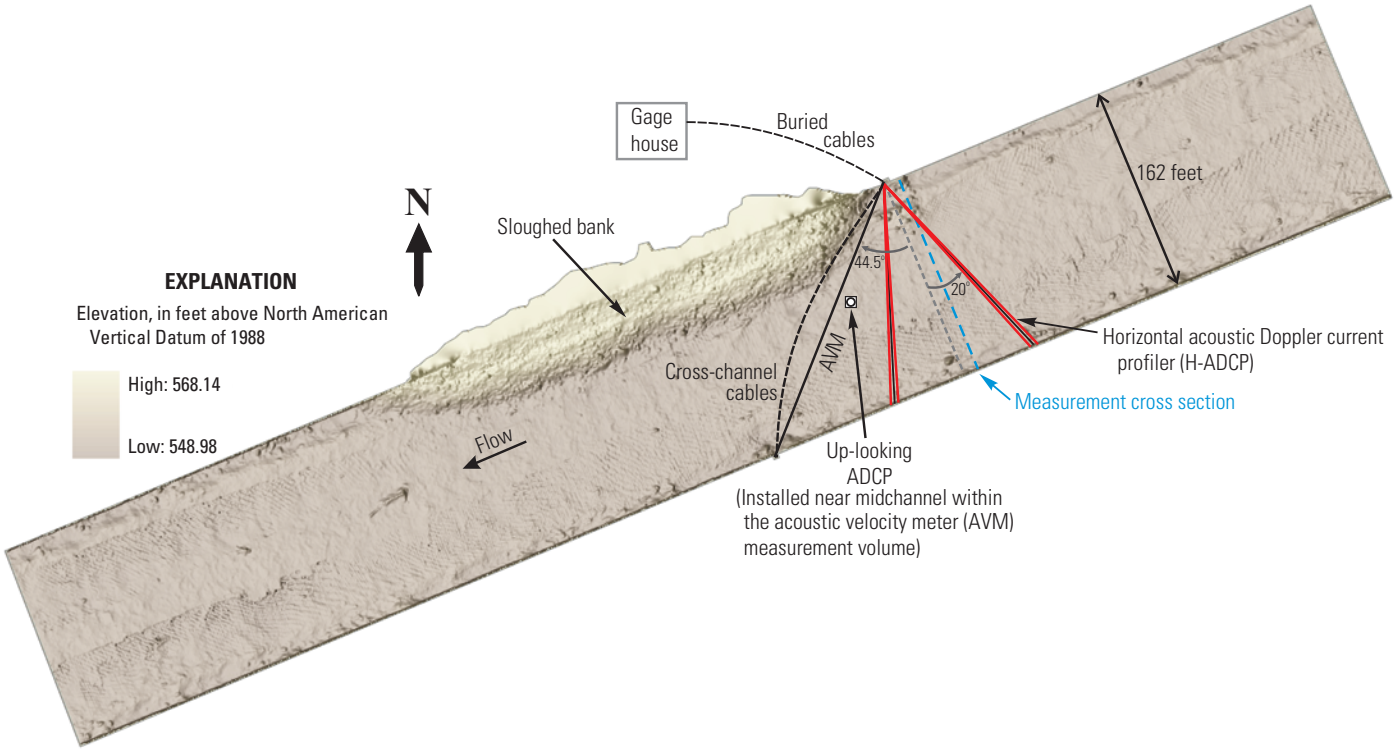

Scientific Investigations Report 2011–5205

U.S. Department of the Interior
U.S. Geological Survey

Cover: Schematic showing the instrument configurations superimposed on the channel bathymetry at the U.S. Geological Survey gaging station on the Chicago Sanitary and Ship Canal near Lemont, Illinois.

Comparison of Index Velocity Measurements Made With a Horizontal Acoustic Doppler Current Profiler and a Three-Path Acoustic Velocity Meter for Computation of Discharge in the Chicago Sanitary and Ship Canal near Lemont, Illinois

By P. Ryan Jackson, Kevin K. Johnson, and James J. Duncker

Prepared in cooperation with the Chicago District of the U.S. Army Corps of Engineers

Scientific Investigations Report 2011–5205

U.S. Department of the Interior
U.S. Geological Survey

U.S. Department of the Interior
KEN SALAZAR, Secretary

U.S. Geological Survey
Marcia K. McNutt, Director

U.S. Geological Survey, Reston, Virginia: 2012

Suggested citation:
Jackson, P.R., Johnson, K.K., and Duncker, J.J., 2012, Comparison of index velocity measurements made with a horizontal acoustic Doppler current profiler and a three-path acoustic velocity meter for computation of discharge in the Chicago Sanitary and Ship Canal near Lemont, Illinois: U.S. Geological Survey Scientific Investigations Report 2011–5205, 42 p.

Contents

Figures

Tables

Conversion Factors

Multiply	By	To obtain
	Length	
foot (ft)	0.3048	meter (m)
meter (m)	3.281	foot (ft)
mile (mi)	1.609	kilometer (km)
	Flow rate	
foot per second (ft/s)	0.3048	meter per second (m/s)
cubic foot per second (ft^3/s)	0.02832	cubic meter per second (m^3/s)
mile per hour (mi/h)	1.609	kilometer per hour (km/h)

Temperature in degrees Celsius (°C) may be converted to degrees Fahrenheit (°F) as follows:
°F=(1.8×°C)+32

Vertical coordinate information is referenced to the North American Vertical Datum of 1988 (NAVD 88).

Instrument and data frequencies are give in hertz (Hz).

Specific conductance is given in microsiemens per centimeter at 25 degrees Celsius (µS/cm at 25 °C).

Salinity is given in parts per thousand (ppt).

Comparison of Index Velocity Measurements Made With a Horizontal Acoustic Doppler Current Profiler and a Three-Path Acoustic Velocity Meter for Computation of Discharge in the Chicago Sanitary and Ship Canal near Lemont, Illinois

By P. Ryan Jackson, Kevin K. Johnson, and James J. Duncker

Abstract

The State of Illinois' annual withdrawal from Lake Michigan is limited by a U.S. Supreme Court decree, and the U.S. Geological Survey (USGS) is responsible for monitoring flows in the Chicago Sanitary and Ship Canal (CSSC) near Lemont, Illinois as a part of the Lake Michigan Diversion Accounting overseen by the U.S. Army Corps of Engineers, Chicago District. Every 5 years, a technical review committee consisting of practicing engineers and academics is convened to review the U.S. Geological Survey's streamgage practices in the CSSC near Lemont, Illinois. The sixth technical review committee raised a number of questions concerning the flows and streamgage practices in the CSSC near Lemont and this report provides answers to many of those questions. In addition, it is the purpose of this report to examine the index velocity meters in use at Lemont and determine whether the acoustic velocity meter (AVM), which is now the primary index velocity meter, can be replaced by the horizontal acoustic Doppler current profiler (H-ADCP), which is currently the backup meter.

Application of the AVM and H-ADCP to index velocity measurements in the CSSC near Lemont, Illinois, has produced good ratings to date. The site is well suited to index velocity measurements in spite of the large range of velocities and highly unsteady flows at the site. Flow variability arises from a range of sources: operation of the waterway through control structures, lockage-generated disturbances, commercial and recreational traffic, industrial withdrawals and discharges, natural inflows, seiches, and storm events. The influences of these factors on the index velocity measurements at Lemont is examined in detail in this report. Results of detailed data comparisons and flow analyses show that use of bank-mounted instrumentation such as the AVM and H-ADCP appears to be the best option for index velocity measurement in the CSSC near Lemont. Comparison of the rating curves for the AVM and H-ADCP demonstrates that the H-ADCP is a suitable replacement for the AVM as the primary index velocity meter in the CSSC near Lemont.

A key component to Lake Michigan Diversion Accounting is the USGS gaging station on the CSSC near Lemont, Illinois. The importance of this gaging station in monitoring withdrawals from Lake Michigan has made it one of the most highly scrutinized gaging stations in the country. Any changes in streamgaging practices at this gaging station requires detailed analysis to ensure the change will not adversely affect the ability of the USGS to accurately monitor flows. This report provides a detailed analysis of the flow structure and index velocity measurements in the CSSC near Lemont, Illinois, to ensure that decisions regarding the future of this streamgage are made with the best possible understanding of the site and the characteristics of the flow.

Introduction

The construction of the Chicago Sanitary and Ship Canal (CSSC) in the late 1800s and the subsequent reversal of the Chicago River in 1900 allowed Chicago to overcome its issues with wastewater and flourish as a city. With the construction and subsequent flow reversal came scrutiny of the withdrawals from Lake Michigan and a U.S. Supreme Court decree limiting Illinois' diversion of Great Lakes water. This decree established the need for diversion accounting and continuous measurement of the discharge of water out of Lake Michigan through the CSSC. To ensure that the best engineering practices and technology are being used in diversion accounting, a technical review committee consisting of practicing engineers and academics is convened every 5 years to review the U.S. Geological Survey's streamgage practices in the CSSC near Lemont, Illinois (Ill.). With locks and control works throughout the Chicago Area Waterway System (CAWS) and significant influences from industry, the CSSC is a highly

unnatural waterway with continuous perturbations that propagate from the lakefront to the confluence with the Des Plaines River at Lockport Lock and Dam (fig. 1). Continuous and accurate measurement of discharge in the CSSC requires innovative technology, measurement redundancy, and extensive data analysis. This report describes the comparison of index velocity measurements for two types of acoustic velocity meters installed at the U.S. Geological Survey (USGS) gaging station on the CSSC near Lemont, Ill..

The intense scrutiny of the Lake Michigan diversion accounting requires a high degree of accuracy and reliability in the USGS discharge measurements and the methods to compute continuous discharge in the CSSC. Continuity in measurements and methods is very important as technology improves and new instrumentation is deployed. It is critical that, whenever possible, an overlap in instrumentation be provided and proper comparison between instrumentation be made to ensure continuity and consistency of the record. The current primary gage in the CSSC near Lemont, Ill., is an acoustic velocity meter (AVM). This time-of-travel meter measures a bank-to-bank average velocity at a specified depth in the measurement reach (index velocity), which is related to a mean cross-sectional velocity by an index velocity rating. The use of AVMs has declined in recent years, and this technology is being replaced by the horizontal acoustic Doppler current profiler (H-ADCP), also called an acoustic Doppler velocity meter (ADVM). The H-ADCP measures velocity in a series of "cells" at a specified distance in front of the bank-mounted unit. Technical limitations prevent the unit from measuring near either bank (the unmeasured near-bank distance is a function of the unit configuration as well as channel geometry and water depth). Currently, an H-ADCP is the backup gage in the CSSC near Lemont and provides measures of discharge during periods of missing record from the primary gage. The lack of support and replacement parts for the AVM has made it necessary to consider using the H-ADCP as the primary gage with AVM as the backup gage. This report presents a comparison of the index velocity measurements and index ratings for the two instruments during a period of overlapping deployment. In addition, the flow at the site is characterized. The report discusses whether the H-ADCP can reliably function as the primary discharge gage while maintaining the continuity and accuracy of the record.

The unsteadiness and unique flow structure in the CSSC make comparison of instrumentation critical prior to any instrumentation change. The inherent differences in the measurement techniques employed by each instrument may potentially lead to biases in reported discharges. As a part of this comparison, the flow characteristics and unsteadiness in the CSSC near Lemont, Ill., are discussed herein, as are the potential effects of these influences on the reported discharge.

Methods

Data Collection

This section describes the index velocity instrumentation used in both the continuous monitoring gages installed on the CSSC near Lemont, Ill., and the synoptic measurements used to calibrate the instruments and investigate the flow structure and unsteadiness.

Continuous Deployments

The USGS has operated a continuous monitoring gaging station on the CSSC near Lemont, Ill., since 2004. Before this, the station was located near Romeoville, Ill., and was moved in 2004 because of interference from the electronic fish barrier operated by the U.S. Army Corp of Engineers (Kevin K. Johnson, U.S. Geological Survey, written commun., 2011). The installation includes a three-path Accusonic ORE 7510 GS acoustic velocity meter (AVM), a Teledyne RD Instruments Channel Master acoustic Doppler velocity meter (H-ADCP) with upward-looking acoustic stage sensor, a ParaScientific pressure sensor (PS-2), a staff gage, two Campbell Scientific electronic dataloggers (CR10X), a high-data-rate satellite transmitter (DCP), and a Sierra Wireless Raven XT Modem. The gaging station is on the right bank in a relatively straight reach with vertical walls, a channel top width of about 162 ft, and mean depth of about 25 ft (fig. 2). The station is in an area of the CSSC where the dolomite bedrock did not extend to the land surface, so set blocks were placed atop the bedrock to form the top part of the canal walls. Along the right bank within the measurement section of the AVM, the set block retaining wall has collapsed, and a significant amount of earth and rock has sloughed into the canal. The year of the collapse is unknown, but it occurred before gage installation. Heavy barge traffic required that the AVM transducers and H-ADCP be mounted in notches cut into the canal walls to protect the instrumentation.

The AVM transmits sound 229.1 ft between transducers on opposite banks at an oblique angle (44.5 degrees) to the channel orientation, and the difference in the traveltime of the sound pulses traveling with and against the flow is directly related to the mean velocity of the water in the cross section. Because the transducers are integrated into the wall of the canal, the full width of the canal is sampled. To provide a better estimate of depth-averaged flow than can be obtained with a single transducer, three transducer sets are mounted at elevations of 570.2, 565.0, and 559.6 ft (NAVD 1988) for paths 1, 2, and 3, respectively (fig. 3). The AVM requires cables to be laid along the riverbed between the transducers at opposite banks, making the instrument susceptible to damage from boat traffic and debris moving along the bed and creating a liability in data continuity. The cables have been severed once since the installation of the system in 2004, and commercial divers were required for repair.

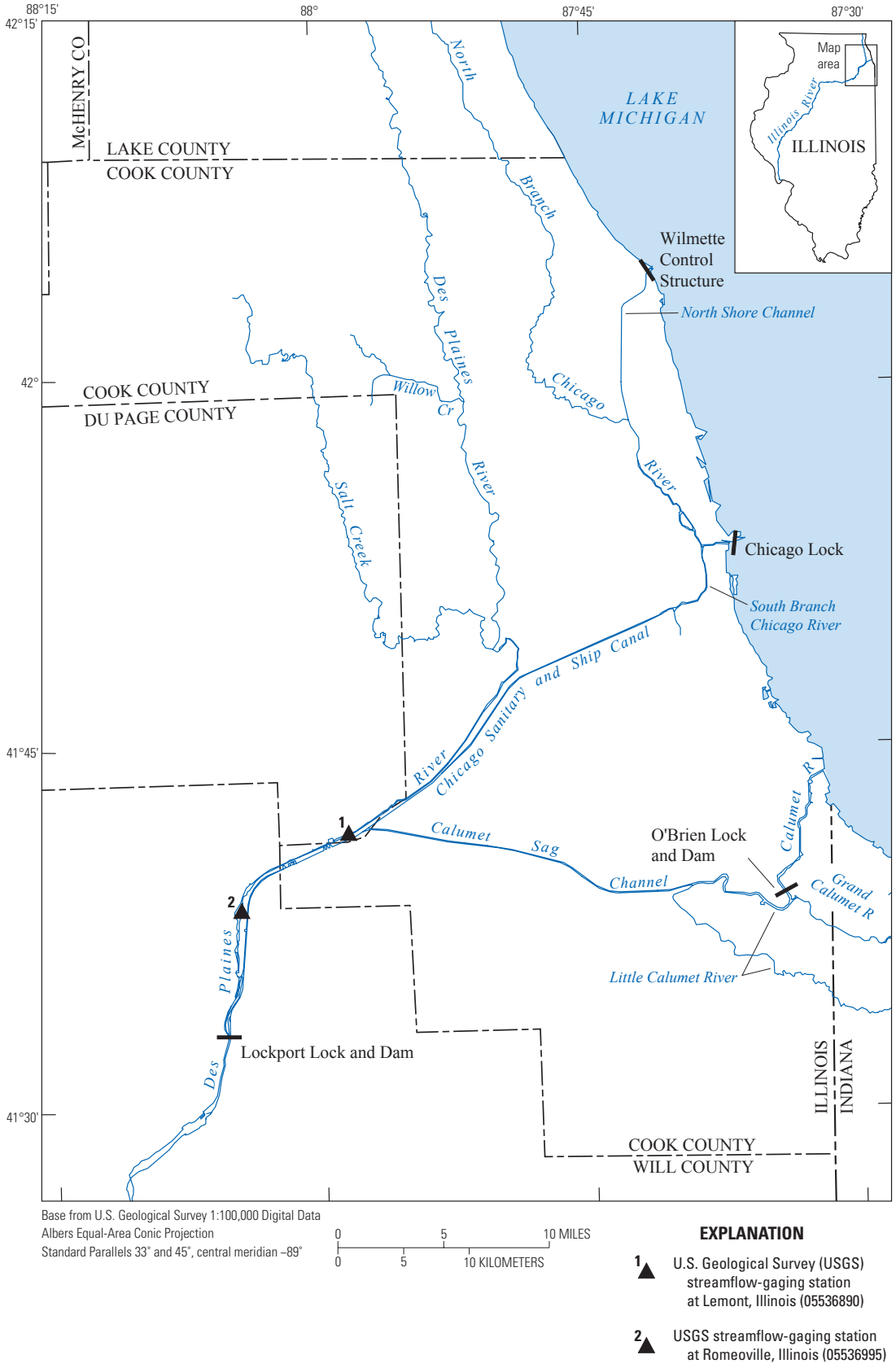

Figure 1. Map of the Chicago Area Waterway System (CAWS) showing the Chicago Sanitary and Ship Canal (CSSC), Calumet Sag Channel, North Branch Chicago River, Little Calumet River, Grand Calumet River, and the other waterways in and near Chicago, Illinois.

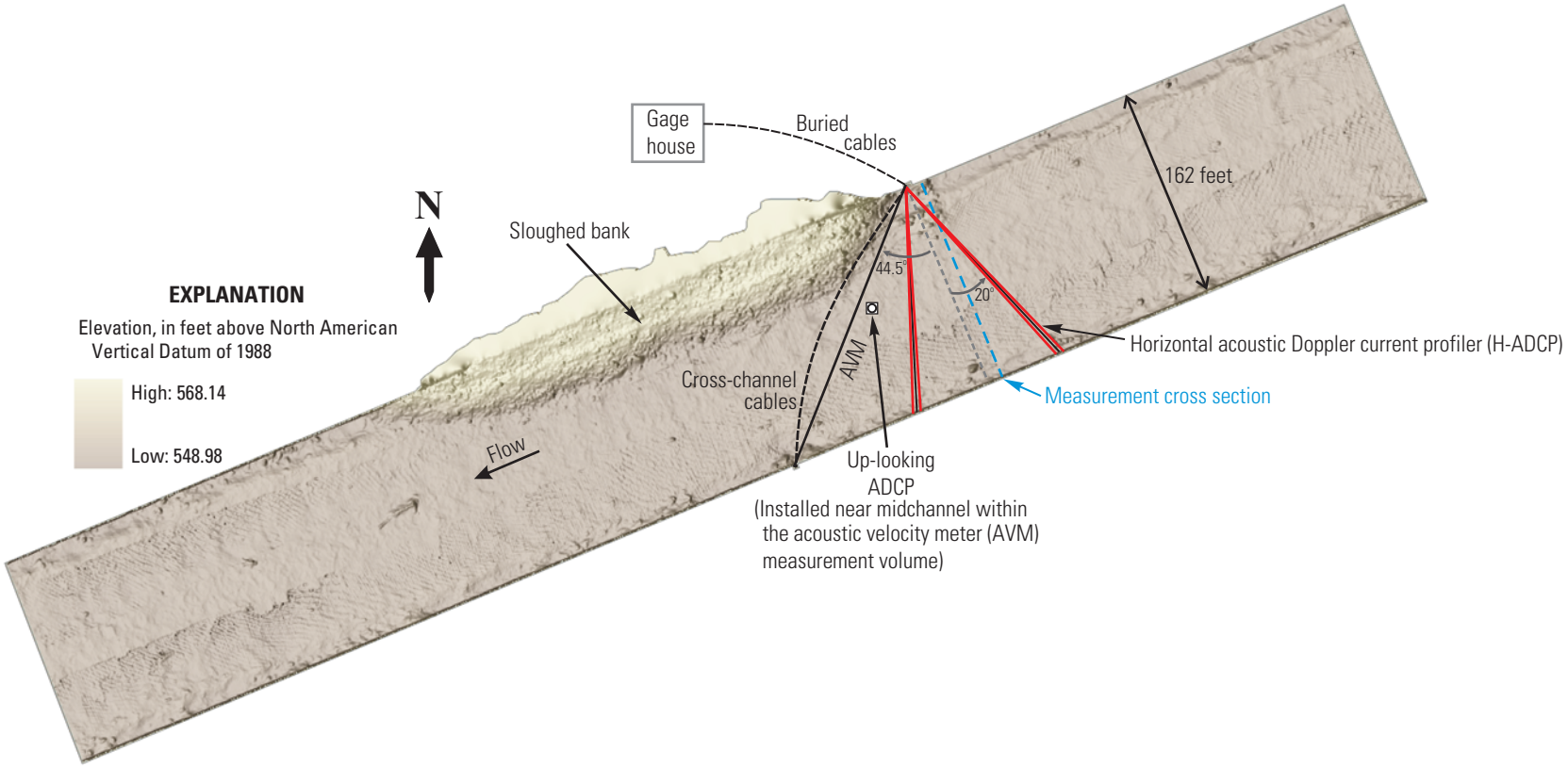

Figure 2. Schematic showing the instrument configurations superimposed on the channel bathymetry at the U.S. Geological Survey gaging station on the Chicago Sanitary and Ship Canal near Lemont, Illinois.

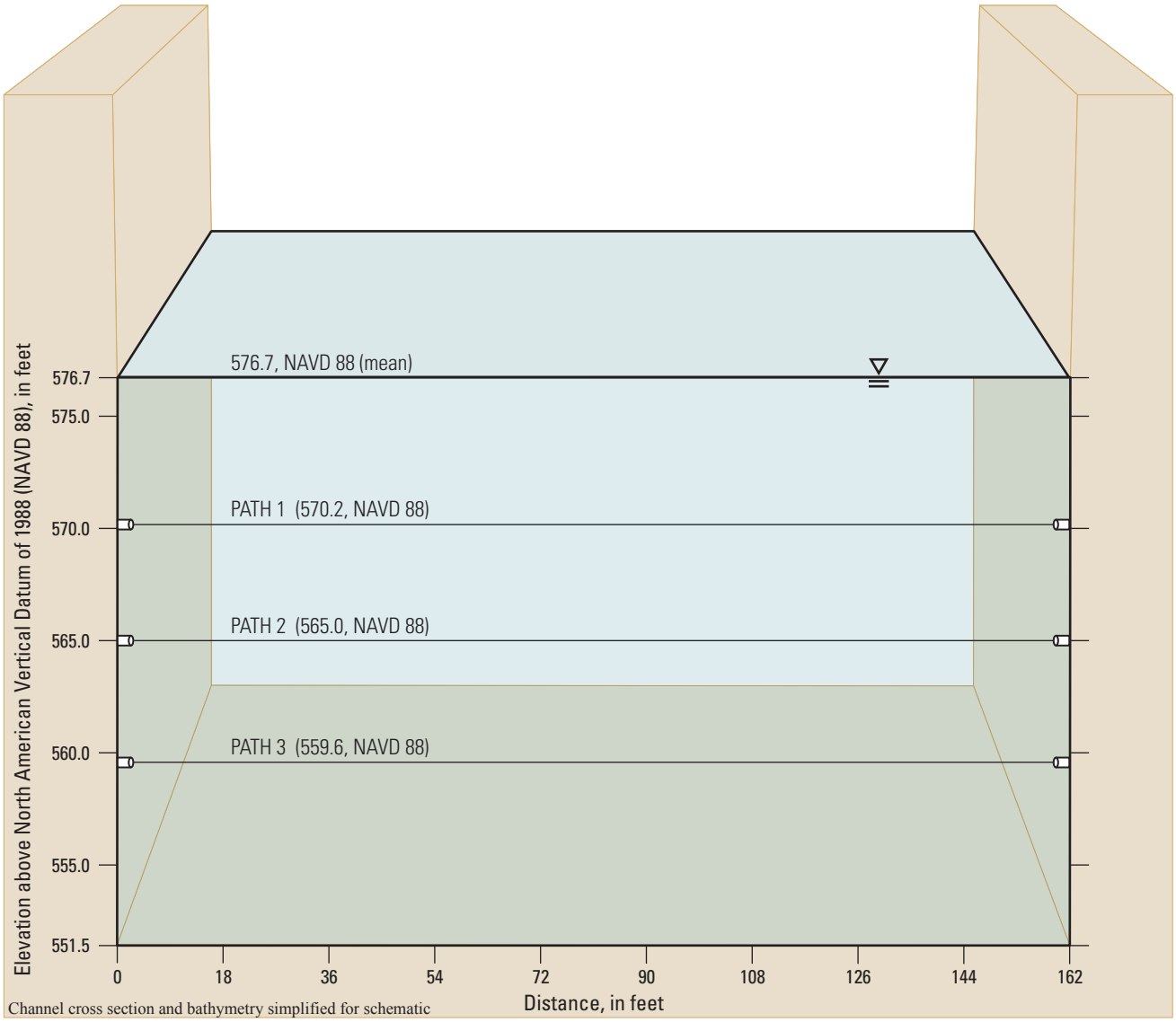

Figure 3. Schematic of the channel cross section showing the three paths of the acoustic velocity meter (AVM) at the U.S. Geological Survey gaging station on the Chicago Sanitary and Ship Canal near Lemont, Illinois (looking upstream)..

The Channel Master H-ADCP requires only one set of bank-mounted transducers and does not require cross-channel cables. The H-ADCP utilizes the acoustic principle of the Doppler shift to measure water velocity. The H-ADCP is oriented perpendicular to the flow, and sound is transmitted out into the channel from two transducers along 20-degree divergent beams and is reflected and scattered by particles in the water (fig. 4). The moving particles reflect some sound back to the unit, which records the frequency of the sound and the time since the emitted pulse. The frequency of the returning sound is different from that of the emitted pulse because of the speed of the particles (Doppler shift). By using multiple beams and range gating based on timing of return pulses, the instrument computes a two-dimensional velocity vector for a series of segments (called cells) across the channel at the elevation of the instrument. Because the instrument is both a transmitter and receiver, a segment of data close to the face of the instrument (called the blanking region) is lost owing to acoustic ringing. On the opposite bank, the divergent beams impinge on the canal walls at an angle of 20 degrees, causing a loss of data (6 percent of the channel width or about 10 ft) owing to the phenomenon of side-lobe interference. Therefore, unlike the AVM, the H-ADCP does not measure the full width of the flow and measures along only one path in the vertical (565.1 ft; NAVD 1988). Theoretically, these differences could lead to potential biases in the computed discharge under certain flow conditions. The instrument is configured such that the measured section is broken into 9 cells with equal widths of 15 ft (fig. 4). The first cell starts 15 ft from the right bank (looking downstream) to accommodate the blanking region and the last cell ends 12 ft from the left bank to allow for the side-lobe interference region.

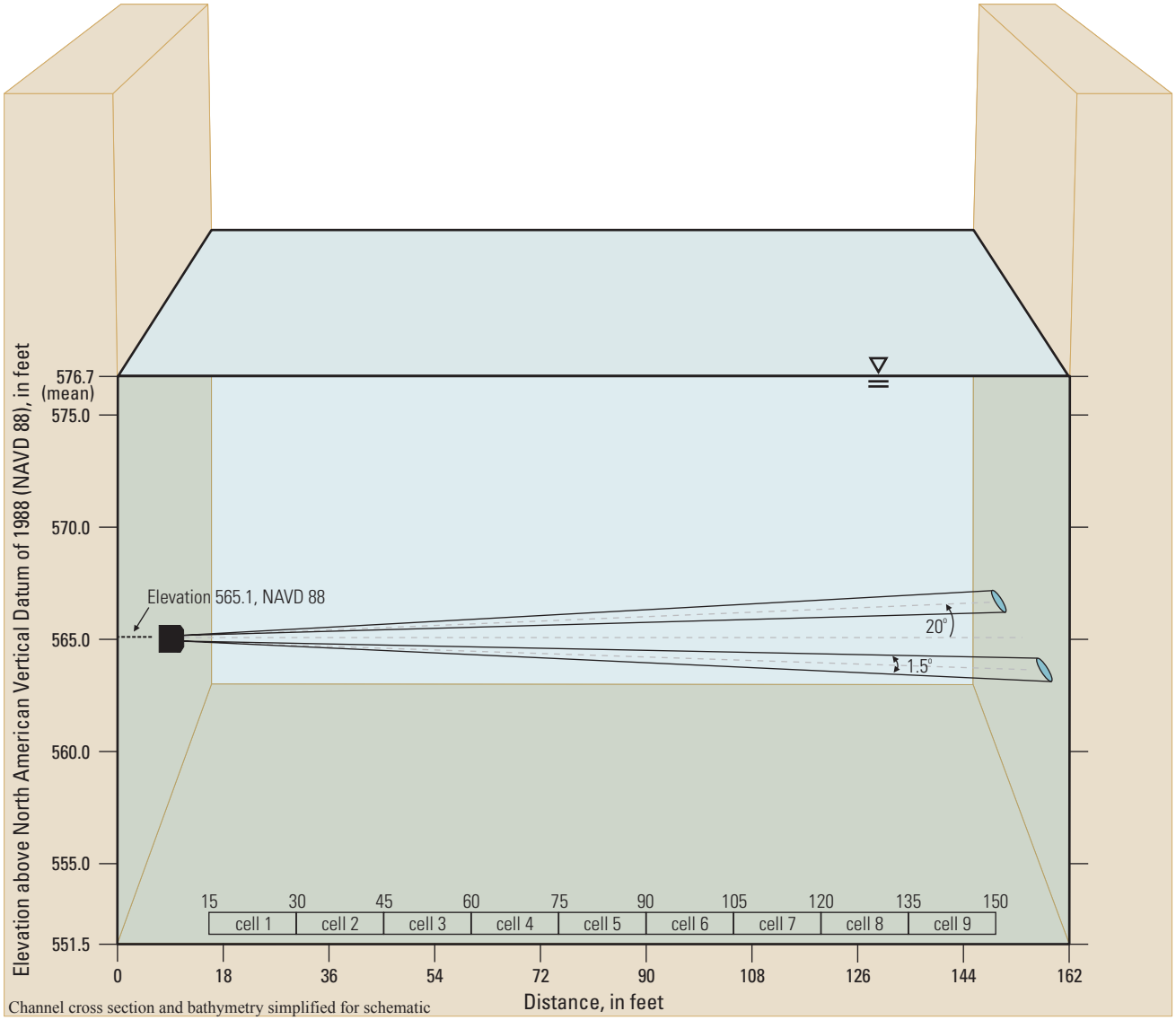

Figure 4. Schematic of the horizontal acoustic Doppler current profiler (H-ADCP) deployed at the U.S. Geological Survey gaging station on the Chicago Sanitary and Ship Canal near Lemont, Illinois (looking upstream).

Synoptic and Short-Term Deployments

The AVM and H-ADCP are both calibrated by relating the index velocities measured by the AVM and H-ADCP to a mean cross sectional velocity (discharge/rated area) determined from a discharge measurement, which is made with an acoustic Doppler current profiler (ADCP) deployed from a moving boat that traverses the canal from bank to bank (hereafter called a boat-mounted ADCP or BM-ADCP). Typically, a 600- or 1,200-kHz Teledyne RDI Rio Grande ADCP is used and is often integrated with a Trimble AG132 differential global positioning system (GPS) for georeferencing of the velocity data. A manned boat on a tag line is typically used for precise control, though remote-controlled boats have been used at this site on occasion. Using the same principles as the H-ADCP, the four-beam BM-ADCP can compute three-dimensional velocity profiles over a zone of the water column below the instrument (fig. 5). This is done while the boat is moved across the canal, allowing the flow field across the channel and channel bathymetry to be measured. The instrument uses either bottom-tracking or GPS to track its location as the boat traverses the channel. Using open-channel flow theory to account for unmeasured areas near the banks, bed, and surface, one can compute the discharge by integrating across the section (Mueller and Wagner, 2009). In addition to a reliable measurement of the total discharge, the moving-boat ADCP measurements yield valuable high-resolution, three-dimensional velocity data that can be used to examine the flow structure at or near the gaging station. A typical discharge measurement takes less than 1 hour to complete, and these measurements are made routinely throughout the year (approximately every 8 weeks) and during periods of high flow.

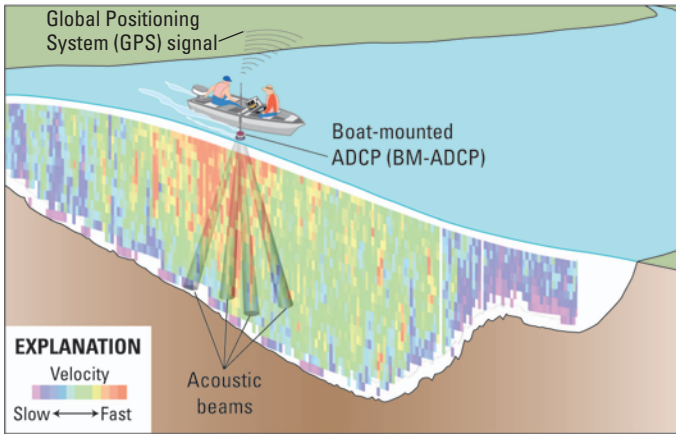

Figure 5. Drawing showing a moving-boat discharge measurement with a boat-mounted acoustic Doppler current profiler (BM-ADCP) and differential global positioning system (GPS) and the resulting velocity magnitude data in the cross section.

To examine the vertical velocity distribution at the site, a bottom-mounted, up-looking ADCP (Teledyne RDI 600-kHz Rio Grande) was deployed approximately midchannel in the path of the AVM in May 2008 for several days and redeployed from March 2009 to June 2010. This stationary instrument continuously measures three-dimensional velocity profiles in the water column above the unit (fig. 6). This unit was tethered to shore with a safety line and communication and power cable, enabling retrieval of the instrument, data logging, and a continuous source of power. In addition, a string of six temperature and conductivity probes was deployed within the notch on the right bank to determine whether any stratified conditions exist at this site. Jackson and others (2008) discovered density currents driven by salinity differences from road-salt runoff at upstream sites in the CAWS near Lake Michigan. Data from the up-looking ADCP was logged to a tablet personal computer while the DCP, phone modem, and data loggers recorded and transmitted data from the thermistors and conductivity sensors.

Data Processing

Index Velocity Computations

The basis of index velocity ratings lies in the ability to relate, through an empirical relation, the velocity at a point or section within a channel, V_{index}, to the mean velocity of the rated cross section defined as $V_{mean} = Q_{measured}/A_{rated}$, where A_{rated} is the rated area of the cross section defined by the stage-area rating curve and $Q_{measured}$ is the measured discharge. The continued success of this rating curve is dependent on the repeatability of the flow structure and, ultimately, the repeatability of the index velocity in the cross section for a given discharge. If the flow structure differs substantially within the measurement volume for the same discharge, the rating will fail to produce a meaningful relation. Index velocity ratings have found use in tidal systems, highly controlled systems with locks and dams, and in surface water systems with significant backwater effects. Unlike a more commonly used stage-discharge rating, index velocity ratings can account for backwater effects and can overcome hysteresis, which can occur in stage-discharge ratings (Morlock and others, 2002). However, hysteresis in index velocity ratings is possible in tidally affected areas (Ruhl and Simpson, 2005).

Calibration Measurements

The index velocity ratings for the instruments in the CSSC near Lemont were developed through calibration measurements made concurrently with the continuous monitoring. For a range of flows, the discharge was measured at or near the index velocity meters by using a BM-ADCP and following standard USGS measurement procedures outlined in Mueller and Wagner (2009). The discharge reported for each measurement was then divided by the rated area determined from the stage-area rating (using a time-weighted mean stage for the measurement period) to compute V_{mean}. A regression was performed between V_{mean} and V_{index} to determine the index velocity rating. This rating is continually checked by making routine and event-driven discharge measurements at the site and checking the measurement against the rating.

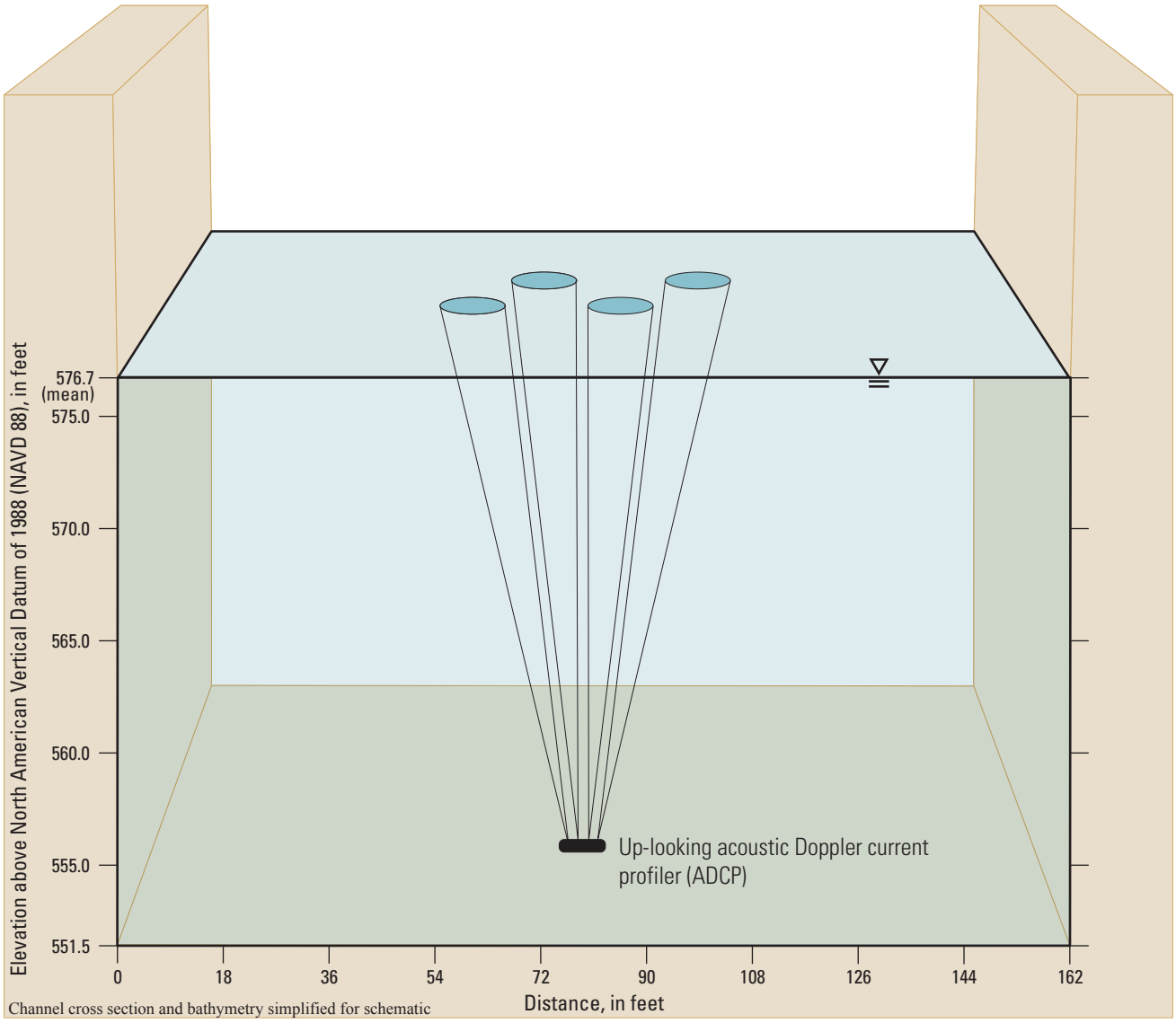

Figure 6. Schematic of the up-looking acoustic Doppler current profiler deployed near midchannel at the U.S. Geological Survey gaging station on the Chicago Sanitary and Ship Canal near Lemont, Illinois.

Acoustic Velocity Meter (AVM)

At the USGS gaging station on the CSSC near Lemont, Ill., the AVM reports the mean water velocity along each of the three acoustic paths at 2-minute and 10-minute intervals. The actual sampling frequency is faster than this (about 1 Hz), but the data are averaged over 2-minute and 10-minute intervals for each path to reduce the noise and yield an accurate mean velocity for each path. Though both values are logged, the 10-minute average velocity is used in the computation of the rated discharge to reduce variability in measurements.

If all three paths report a valid velocity for the 10-minute sampling period, the AVM index velocity V_{AVM} is computed as the arithmetic mean of the velocities for each of the three paths:

$$V_{AVM} = \frac{1}{n_p} \sum_{i=1}^{n_p} V_i \qquad (1)$$

where

V_i is the 10-minute average velocity of the i^{th} acoustic path, and

n_p is 3 for valid data on all three paths.

If any individual path returns a missing velocity (no measurement made) or invalid velocity (erroneous as determined internally by the AVM) during the 10-minute sampling period, then the reported mean for that path is not valid and is reported as missing data. If one or two of the paths report missing data for the 10-minute average, path coefficients are multiplied by the remaining good path velocities prior to arithmetic averaging to determine V_{AVM}. Path coefficients are used to correct V_{AVM} for the effect of missing or invalid data. Path coefficients were determined by using the 10-minute path velocities from December 19, 2005, to January 3, 2008. Approximately 93,000 values (86 percent of record) were used, which comprised all valid and non-zero path velocities for each of the three paths. The AVM path coefficients C_i were determined by dividing the three path arithmetic mean V_{AVM} by the 10-minute average velocity along each path:

$$\frac{V_{AVM}}{V_i} = C_i \tag{2}$$

where

i = 1, 2, 3.

The approximately 93,000 path coefficients for each path were averaged to define a single path coefficient for each path of the AVM. The computed path coefficients for AVM paths 1, 2, and 3 are 0.9300, 1.0134, and 1.0836, respectively. In the event that all three path velocities are invalid for a 10-minute averaging interval, V_{AVM} for that time period is left blank and reported as missing data.

Horizontal-ADCP (H-ADCP)

At the USGS gaging station on the CSSC near Lemont, Ill., the H-ADCP reports the mean water velocity in each of the nine cells across the channel at 1-minute intervals. The actual sampling frequency is faster than this (about 1 Hz), but the data are averaged over 1-minute intervals for each cell to reduce the noise.

The H-ADCP index velocity $V_{H\text{-}ADCP}$ is computed as the arithmetic average of the nine cross-channel cell velocities,

$$V_{H-ADCP} = \frac{1}{n_c}\sum_{i=1}^{n_c} V_{b_i} \tag{3}$$

where

V_{bi} is the 1-minute average cell velocity in the i^{th} cell, and

n_c equals 9 for valid data in all cells.

If data from any cell are invalid (as determined by internal screening in the instrument), the average is computed from the remaining cells with no coefficients applied to account for the missing cells. In the event that all nine cell velocities are invalid, $V_{H\text{-}ADCP}$ for that time period is left blank and reported as missing data.

Stage-Area Rating

Index velocity ratings require a stage-area rating curve to transform a measured stage or gage height (water-surface elevation relative to a gage datum) to cross-sectional area prior to computation of discharge. Stage-area ratings are built from a cross-section survey and must be continually checked to ensure that the cross section is not changing. The stage-area rating for the CSSC near Lemont has been stable since installation of the gage in 2004. The rating is occasionally checked by using data collected during discharge measurements at the same cross section as defined in the stage-area rating (see fig. 2). The stage-area rating for the CSSC at Lemont, Ill., is defined as

$$A_{CSSCL} = 139.83\, G_{CSSCL} + 670.39 \tag{4}$$

where

A_{CSSCL} is the rated area for the CSSC near Lemont, and

G_{CSSCL} is the gage height at CSSC near Lemont.

A report containing more detailed information on the development of the stage-area rating curve for the CSSC near Lemont is currently (at the time of this publication) under review (Kevin K. Johnson, U.S. Geological Survey, written commun., 2011).

Discharge Computation

Once V_{index} is determined (that is, V_{AVM} or $V_{H\text{-}ADCP}$), the index velocity rating for the instrument is used to determine the mean cross sectional velocity V_{mean}. The observed gage height is used in conjunction with the stage-area rating for the site to determine the rated area of the cross section. The rated discharge Q_{rated} is then computed as the product of the mean cross-sectional rated velocity V_{mean} and the rated area A_{rated}.

Results

Flow Characterization

This section is dedicated to analysis of the observed flows in the Chicago Sanitary and Ship Canal near Lemont, Ill. The analysis evaluates in detail the sampling configuration of the instruments and potential effects of the flow structure on the measured index velocities for each instrument.

Velocity Magnitude and Direction

Distribution of Observed Velocities

Velocity data from the AVM and H-ADCP were analyzed to determine the range of flows observed in the CSSC near Lemont, Ill. The data used in the analysis consisted of 10-minute data from the AVM for November 2006–January 2010 and 10-minute data from the H-ADCP for the same period. Individual velocities observed for each path of the AVM and each cell of the H-ADCP were analyzed independently.

For the selected period for analysis, the CSSC near Lemont, Ill., exhibits a skewed distribution of flow velocities, with the greatest occurrence of velocities in the 0.5- to 0.75-ft/s range. To a lesser extent, velocities in the range 3.5 to 4.0 ft/s were also relatively common (figs. 7 and 8). Both the AVM and the H-ADCP registered this skewed distribution in all paths and cells (except cell 9 of the H-ADCP). Both instruments registered negative velocities and velocities as high as 5 ft/s; however, the range of observed velocities was slightly wider for the H-ADCP, likely because of the smaller measurement volume used in this system (15-ft cell width for the H-ADCP compared to a 162-ft channel width for the AVM). This skewed distribution is likely caused by the operation of the powerhouse and lock at Lockport, Ill. The primary peak at 0.5 to 0.75 ft/s arises from "normal" power generation at the powerhouse, when about 2,000 ft^3/s is discharged through the turbines. However, in advance of storms, the Metropolitan Water Reclamation District of Greater Chicago (MWRDGC) will draw down the canal to provide storage by increasing flow through the powerhouse and opening sluice gates at the powerhouse and at the controlling works upstream of Lockport. These rapid drawdown events in the canal and the flood events that follow appear to generate a range of flows with peak velocities around 4 ft/s. A third, hardly perceptible peak occurs in the range 2 to 3 ft/s, and this may be associated with flows resulting from lockages and/or operational changes in power generation and flow structures.

The highest velocities occur nearest the surface and within H-ADCP cells 5, 6, and 7. With the exception of cell 9, which exhibits a low bias over the entire range of observed flows (discussed in detail later in this report), the high flows appear to be biased to the left bank, as do the negative flows. Detailed discussions of the transverse velocity distribution and flow reversals are also presented later in this report.

Primary and Secondary Flows and Flow Angle

The index velocity methods applied in the CSSC near Lemont utilize the streamwise component of the velocity (parallel to the course of the river) in the computation of the index velocity. For these techniques to be effective, flow at the chosen sites must be relatively unidirectional over the range of flows at the sites. Uncertainty in the index velocity rating can be introduced if the flow direction (or direction of primary velocity) within the measurement volume of the index velocity meter changes under similar discharge conditions. Therefore, from the 61 discharge measurements made before April 2010, a subset of 29 was selected to complete a detailed analysis of the flow direction near Lemont. The selected measurements included GPS data and valid compass calibrations (used to georeference velocity data), requirements for a proper analysis. These measurements were collected and processed by use of USGS standard methods (Mueller and Wagner, 2009).

The 29 discharge measurements each consisted of at least 4 transects (but often 8 or more) at a fixed measurement section just upstream of the notch in the right bank (fig. 2). A transect is defined as a single traverse of the instrument from one bank of the river to the alternate bank. By using the Matlab-based program Velocity Mapping Toolbox (VMT; Daniel R. Parsons, University of Leeds, written commun., 2011), the BM-ADCP data for each measurement were mapped to the fixed measurement section and interpolated to a regular grid with horizontal grid node spacing of 0.1 m and vertical grid node spacing equal to the bin size (variable), and flow components were averaged across all transects at each grid node. Flow components computed include streamwise and transverse velocity (as set by the channel orientation near Lemont), primary and secondary velocities defined by both the zero net secondary discharge (ZSD) and Rozovskii (ROZ) definitions (Lane and others, 2000), and vertical velocity. Primary velocity is the component of velocity in the direction that maximizes downstream discharge and minimizes cross-stream discharge for either the whole cross section (ZSD definition) or for each individual velocity profile (ROZ definition). Secondary velocity is the component of velocity perpendicular to the primary velocity in the transverse (or lateral) direction. This analysis yielded an average velocity cross section for each measurement. By using the same procedure, the acoustic backscatter recorded by the ADCP during the measurement was averaged to produce an average backscatter cross section for each measurement. Acoustic backscatter is the intensity of the signal returned to the instrument from particles in the water column and is generally proportional to the concentration and size of particles in the water column (and may be used as a surrogate for suspended sediment with proper calibration). Primary and secondary velocities are used in this analysis to determine the magnitude of flow perpendicular to the direction of discharge. Although not currently used for rating development, these components of flow may help explain some uncertainty in the index velocity rating at Lemont.

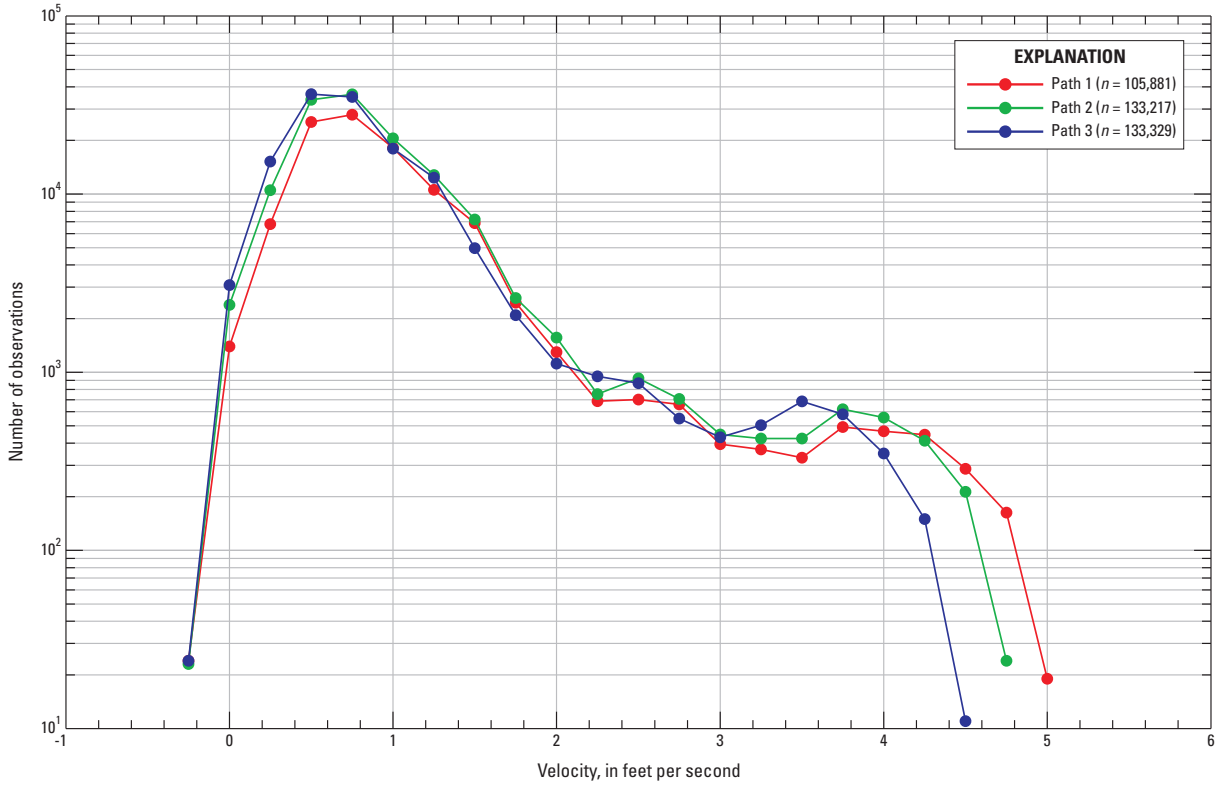

Figure 7. Frequency-distribution diagrams of velocity magnitude observations for each of the three paths of the acoustic velocity meter (AVM) in the Chicago Sanitary and Ship Canal near Lemont, Illinois, December 2005–January 2010.

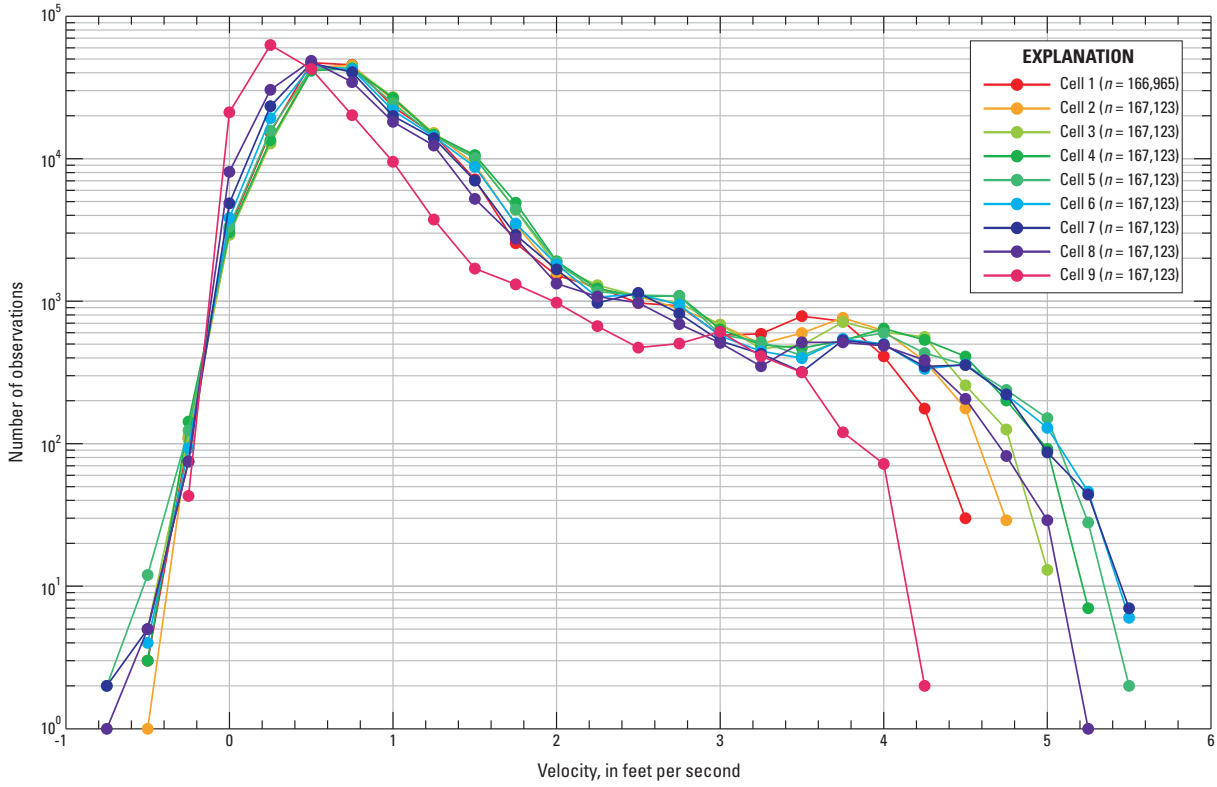

Figure 8. Frequency-distribution diagrams of velocity magnitude observations for each of the nine cells of the horizontal acoustic Doppler current profiler (H-ADCP) in the Chicago Sanitary and Ship Canal near Lemont, Illinois, November 2006–January 2010.

As the discharge and mean velocity in the CSSC near Lemont decreases, the primary flow direction shows greater deviation from the streamwise direction (fig. 9; table 1). Primary flow directions determined by using the zero net secondary discharge method (Lane and others, 2000) were found to deviate from the streamwise direction by as much as 4.3 degrees at very low flows. Flow angles of this magnitude will lead to less than a 1-percent negative bias in the index velocity (errors are proportional to $1-\cos(\theta)$, where θ is the absolute value of the flow angle) as the index velocity meters generally only use the streamwise velocity in the computation of the index velocity. However, it is important to note that the flow angle determined here is an average flow angle determined by rotating the section such that the net secondary discharge is zero. Therefore, individual flow angles at any point in the cross section may be substantially different from that reported here. An index velocity meter samples only a small fraction of the cross section, and if the flow angles vary substantially, the variation will result in greater errors in the measurement of an index velocity.

The magnitude of the secondary velocity increases relative to the primary velocity as the mean velocity decreases in the CSSC near Lemont (fig. 9). On the basis of the 29 discharge measurements analyzed, the greatest ratios of secondary to primary velocity are observed at low flows. For V_{mean} < 0.6 ft/s, secondary velocities increase in magnitude and can exceed 10 percent and be as much as 82 percent of the magnitude of the primary velocity. For V_{mean} > 0.6 ft/s, the secondary velocities are less than 10 percent of the primary velocity, and the ratio further decreases with increasing V_{mean}. Secondary flows can arise from channel curvature, channel confluences, bathymetry, environmental effects such as wind, and stratified flows. The CSSC near Lemont is subject to all these factors.

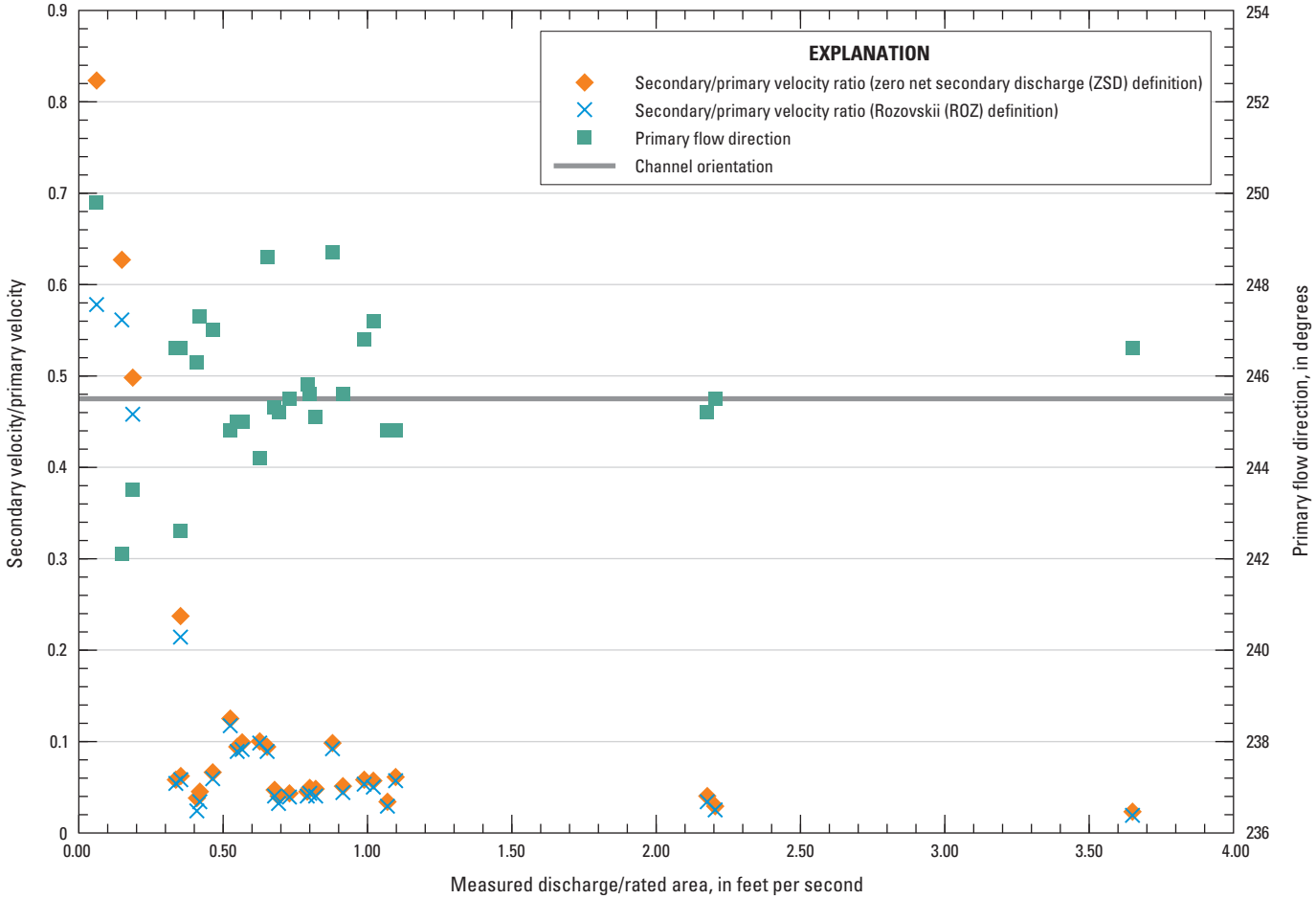

Figure 9. Primary and secondary flows as a function of V_{mean} for the Chicago Sanitary and Ship Canal near Lemont, Illinois.

Table 1. Primary and secondary velocities observed during discharge measurements in the Chicago Sanitary and Ship Canal near Lemont, Illinois.

[$V_{mean} = Q/A_r$, where Q is the measured discharge and A_r is the rated area; ZSD, zero net secondary discharge; ROZ, Rozovskii definitions]

Measurement number	V_{mean}, in cubic feet per second	Secondary/primary velocity ratio (ZSD)	Secondary/primary velocity ratio (ROZ)	Primary flow direction, in degrees from true north	Flow angle[1], in degrees
17	0.35	0.237	0.214	242.6	2.9
23	.99	.058	.053	246.8	−1.3
34	.42	.045	.034	247.3	−1.8
35	.41	.038	.024	246.3	-.8
36	.65	.094	.089	248.6	−3.1
37	.88	.098	.092	248.7	−3.2
38	3.65	.023	.019	246.6	−1.1
39	.57	.099	.091	245	.5
40	1.02	.057	.05	247.2	−1.7
41	1.10	.061	.057	244.8	.7
42	.55	.094	.089	245	.5
43	.63	.1	.098	244.2	1.3
44	.53	.125	.117	244.8	.7
45	.19	.498	.458	243.5	2
46	.06	.823	.578	249.8	−4.3
47	.15	.627	.561	242.1	3.4
48	.69	.04	.032	245.2	.3
49	2.20	.029	.025	245.5	0
50	2.18	.04	.034	245.2	.3
51	1.07	.034	.029	244.8	.7
52	.92	.051	.044	245.6	−.1
53	.82	.048	.04	245.1	.4
54	.73	.043	.039	245.5	0
55	.79	.045	.04	245.8	−.3
56	.80	.049	.043	245.6	−.1
57	.46	.066	.059	247	−1.5
58	.68	.047	.04	245.3	.2
60	.35	.062	.058	246.6	−1.1
61	.34	.058	.054	246.6	−1.1

[1]From streamwise flow direction (245.5 degrees from true north near Lemont, Ill.).

To assess the effect of flow angle and secondary flows on index velocity measurements near Lemont, the percent difference and residuals of the rated discharge from the measured discharge were plotted against the flow angle (figs. 10*A* and 10*B*) and the ratio of secondary and primary velocities (figs. 11*A* and 11*B*). The percent difference data show a weak trend in which errors in the rated discharge increase for larger flow angles and larger secondary to primary velocity ratios. Residual plots have considerable scatter and are generally inconclusive. This relatively simple analysis may help explain why certain measurements do not fall in line with the rating (for example, measurements 45–47). Though the H-ADCP and AVM show the same general trend, the AVM appears to be more susceptible to errors in flows with relatively large flow angles and secondary flows. Individual differences in the rated discharge from the measured discharge for the AVM and H-ADCP can exceed 40 percent at lower discharges (less than about 500 ft^3/s). These errors greatly exceed those computed by using simple geometry and the mean flow angle, indicating that the limited sample volume of the instruments may result in unbalanced and disproportionately large flow angles compared to the overall cross section. However, secondary flows often occur in places where flows are complex, and complex flows are inherently more difficult to accurately measure. The relationship between rated discharge errors and secondary currents (and flow angle) may also be a product of an overall increase in discharge-measurement uncertainty in nonuniform flows.

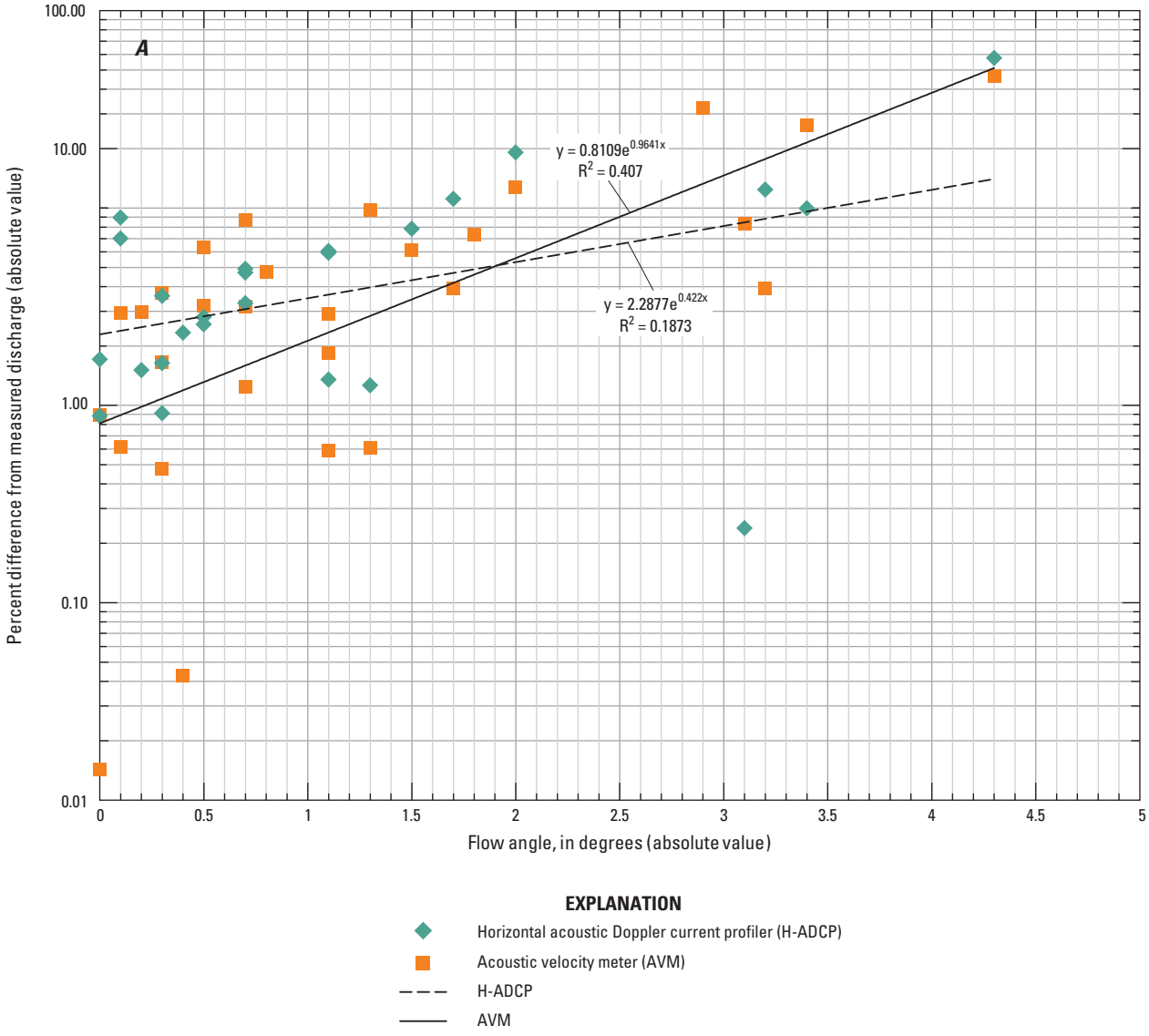

Figure 10*A*. Percent difference from the measured discharge as a function of the flow angle in the Chicago Sanitary and Ship Canal near Lemont, Illinois.

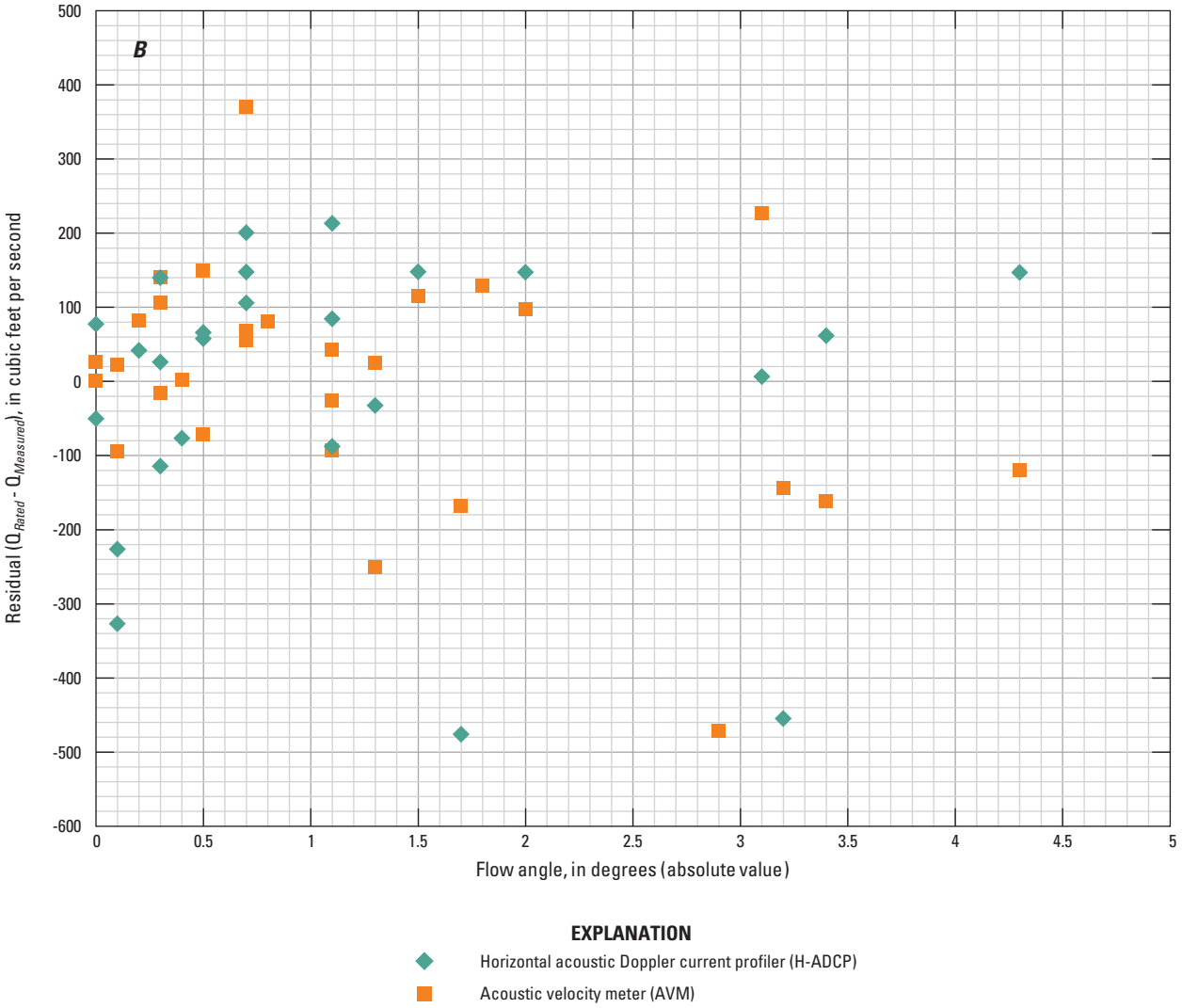

Figure 10*B*. Residuals (rated discharge minus measured discharge) as a function of flow angle in the Chicago Sanitary and Ship Canal near Lemont, Illinois.

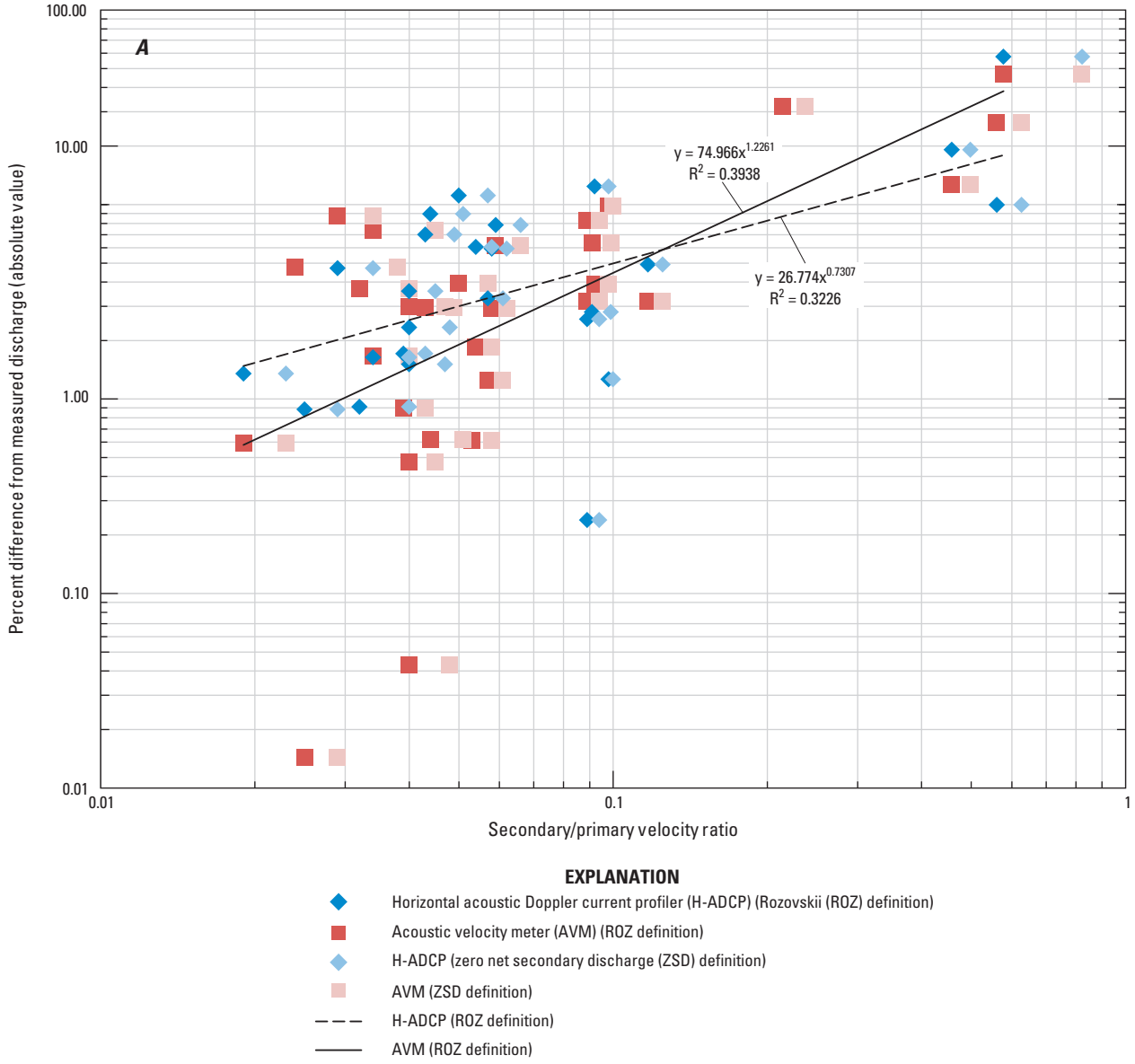

Figure 11*A*. Percent difference from the measured discharge as a function of the secondary to primary velocity ratio in the Chicago Sanitary and Ship Canal near Lemont, Illinois.

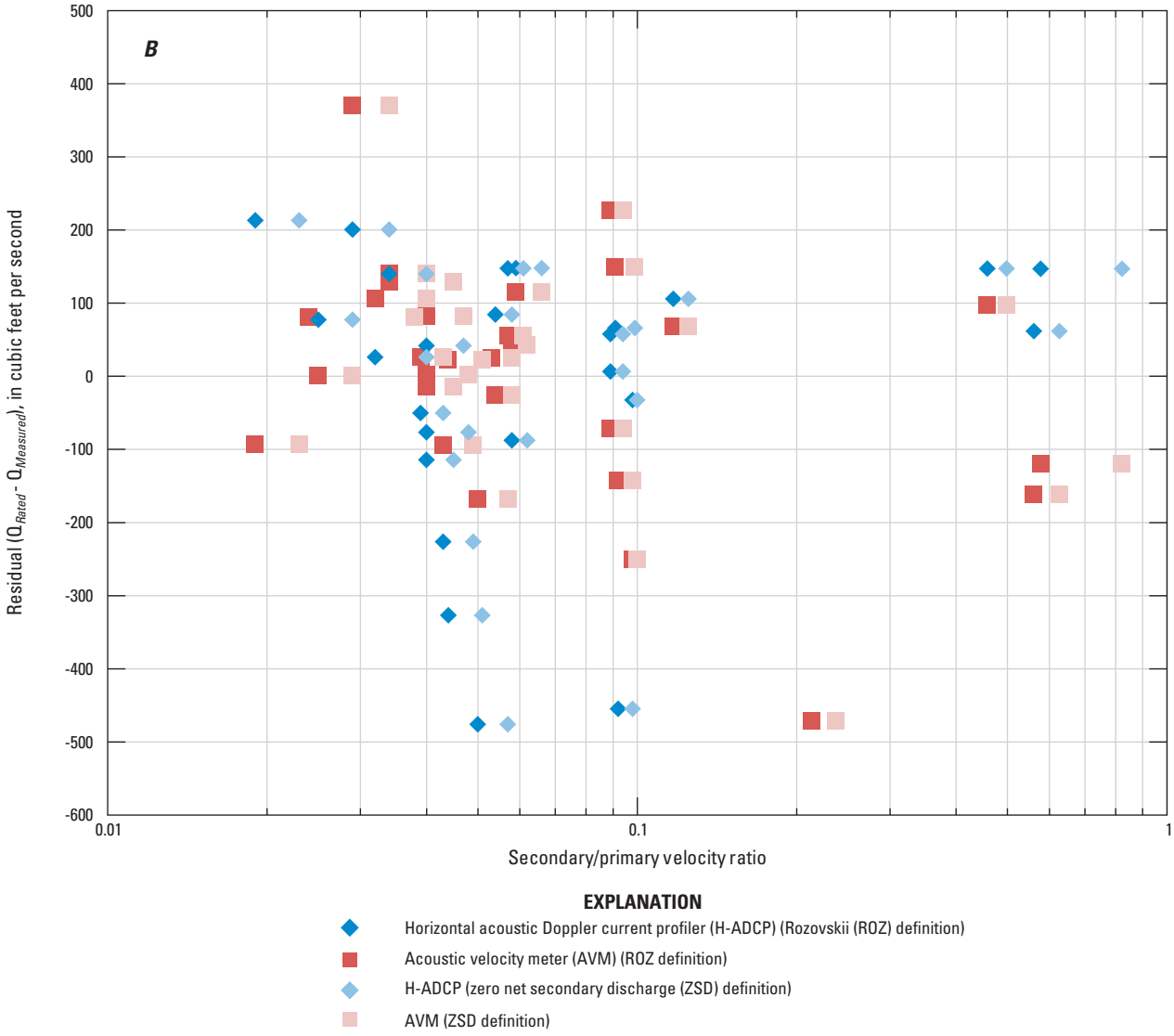

Figure 11*B*. Residuals (rated discharge minus measured discharge) as a function of the secondary to primary velocity ratio in the Chicago Sanitary and Ship Canal near Lemont, Illinois.

Temporal Variability

Frequency Analysis

The flow in the CSSC near Lemont, Ill., is highly variable in response to turbine and sluice gate changes and lockages at Lockport, Chicago Lock and Chicago River Controlling Works, and O'Brien Lock and Dam. In addition, temporal variations in the flow are also caused by variability in barge traffic, sewage-treatment-plant discharge, powerplant cooling-water discharge, industrial intake and discharge, wind, seiches, and tributary inflows. Although some of these processes produce nonperiodic variations in the flow near Lemont, many likely contain some form of periodicity, whether it is a diurnal variation in effluent discharge, routine control-gate changes, or seiche periods set by the flow depth and channel geometry. Pulsing of the flow near Lemont is common and is identifiable in the velocity records of the AVM, H-ADCP, and up-looking ADCP.

Velocity records (2-minute data for the AVM and 1-minute data for the H-ADCP) were examined for the periods October 2007–January 2010 (AVM) and November 2006–January 2010 (H-ADCP) to determine whether any dominant frequencies in the data exist. Power spectra were independently generated for each cell of the H-ADCP and each path of the AVM (fig. 12). Dominant frequencies are evident as local peaks in the power spectrum; these were identified, and the corresponding frequencies were documented.

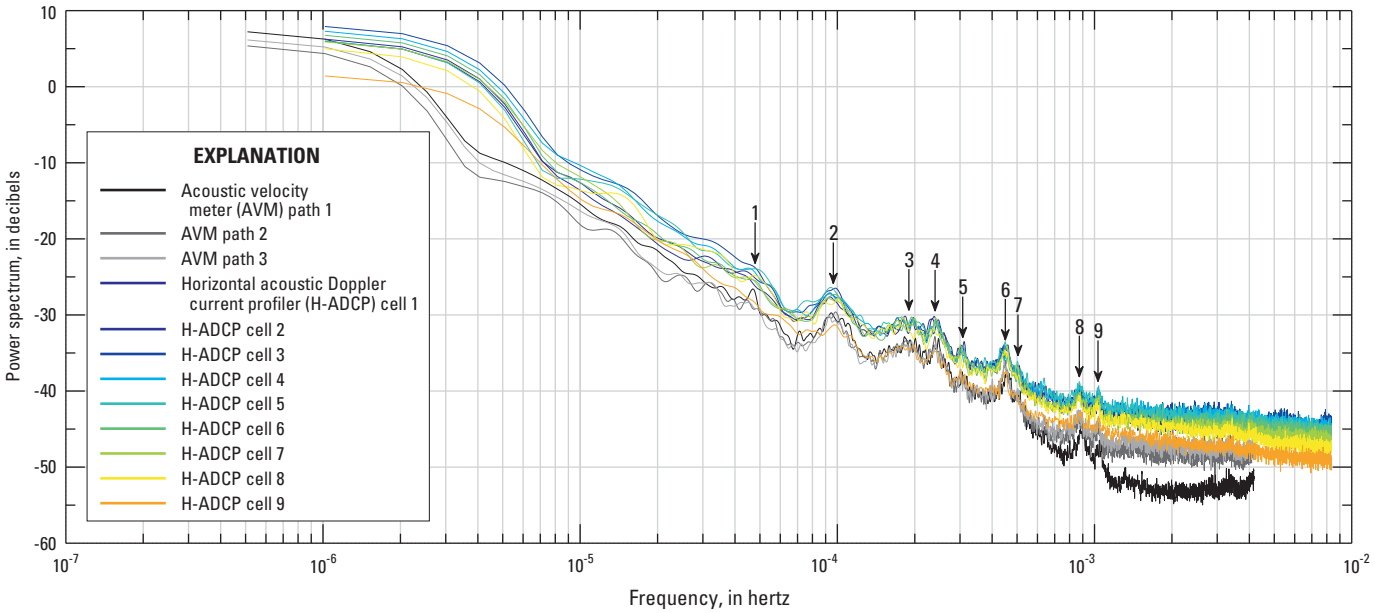

Figure 12. Power spectra for acoustic velocity meter (AVM) path and horizontal acoustic Doppler current profiler (H-ADCP) cell velocity data, November 2006–January 2010, in the Chicago Sanitary and Ship Canal near Lemont, Illinois. (Numbered arrows identify dominant-frequency peaks in the record.)

Although analyzed independently, all paths of the AVM and all cells of the H-ADCP showed numerous dominant frequencies, with corresponding periods in the range of 16.1 to 348.9 minutes (table 2). A total of eight dominant frequencies (peaks 2–9) were identified in all records, and an additional weak peak (peak 1) was identified in some of the H-ADCP cell data and the AVM path 1 data. The frequencies and periods associated with the peaks identified in figure 12 are listed in table 2. In spite of the higher sampling frequency of the H-ADCP, the high-frequency data (greater than approximately 10^{-3} Hz) appear to be overwhelmed by the noise of the instrument. The plateau of the H-ADCP data at high frequency is indicative of the effect of instrument noise (Anderson and Lohrmann, 1995) and masks oscillations in the data at periods less than about 15 minutes. The AVM data show a similar response at high frequencies, though the noise floor for the AVM is slightly lower than for the H-ADCP.

The CAWS is a closed system with locks and control structures regulating flow on the inlets and outlets of the system. The primary influences on this system with respect to flow unsteadiness are control changes and lockages at Lockport. Lockport Lock and Dam is a large structure with a 39.5-ft head difference across the structure, and changes in flow at Lockport are felt throughout the CAWS. By using shallow-water wave theory, the periods for various seiche modes were computed for the CAWS on the basis of an approximate mean depth and reach length (Dean and Dalrymple, 1984). Because the system has multiple branches, this analysis was performed on each of the three primary arms: Lockport to Wilmette, Lockport to Chicago Lock, and Lockport to O'Brien Lock (see fig. 1). These three reaches have corresponding approximate mean depths of 20.3 ft, 24.9 ft, and 17.4 ft, respectively (computed by using a distance-weighted mean and bathymetry from the USGS and U.S. Army Corps of Engineers). Reach lengths are approximately 50.0 mi, 36.3 mi, and 35.1 mi, respectively. The first 15 seiche modes were computed for each branch of the system. Although an infinite number of modes are theoretically possible, the lower modes are likely present in nature as higher frequency modes are damped out by friction.

Table 2. Dominant frequencies and periods for the acoustic velocity meter (AVM) and horizontal acoustic Doppler current profiler (H-ADCP) velocity data for October 2007–January 2010 (AVM) and November 2006–January 2010 (H-ADCP) in the Chicago Sanitary and Ship Canal near Lemont, Illinois.

Peak number[1]	Frequency (hertz)	Period (minutes)
1	4.777E−05	348.9
2	9.590E−05	173.8
3	1.896E−04	87.9
4	2.408E−04	69.2
5	3.041E−04	54.8
6	4.505E−04	37
7	5.020E−04	33.2
8	8.726E−04	19.1
9	1.035E−03	16.1

[1]Peaks are identified in the spectra presented in figure 12.

At least half of the dominant frequencies identified in the CSSC near Lemont are consistent with seiche modes, and seiches in the Lockport to Wilmette reach appear to make the largest contribution to flow variability near Lemont (fig. 13). Peaks 1, 2, and 4 in the power spectrum (fig. 12) can be explained by the modes 1, 2, and 5 seiches for the Lockport to Wilmette reach. Peak 3 compares well with the Lockport to Wilmette mode 4 and Lockport to O'Brien mode 3 seiches. Peak 6, a well pronounced peak in both the AVM and H-ADCP data, may be owing to the superposition of the Lockport to Chicago Lock mode 6 seiche and the Lockport to O'Brien mode 7 seiche. Finally, the period associated with peak 9 is equal to the Lockport to Chicago lock mode 14 seiche period. In addition to these seiche modes that are well correlated with the observed periods present in the data, several other modes show reasonably good correlation and may be able to explain the spectrum peaks within the uncertainty of the seiche mode periods.

Flow Variability Owing to Barge Passage

The effect of barge/tow passages through the CSSC near Lemont was investigated by using the up-looking ADCP data from May 2008 and June 2009. Because the up-looking ADCP was placed midchannel, barges passing through the measurement volume can be identified in the data as the flow is disturbed and the beams impinge on the bottom of the vessel, causing a sudden change in the acoustic return. Therefore, the up-looking ADCP data were used to identify the start and end times of a barge passage by marking the start and end times of these disturbances. In addition, because the instrument has four diverging beams and a compass, the orientations of the instrument's beams are known; and by analyzing the intensity of the acoustic returns of each beam at the beginning of each barge disturbance, the direction of travel (that is, upstream or downstream) can be identified. Finally, the ferrous metals in the vessels create a disturbance in the local magnetic field and cause erroneous readings from the compass on the up-looking ADCP during the time of passage when the barge is directly over the ADCP. Therefore, the compass readings are a good indicator of barge/tow passages.

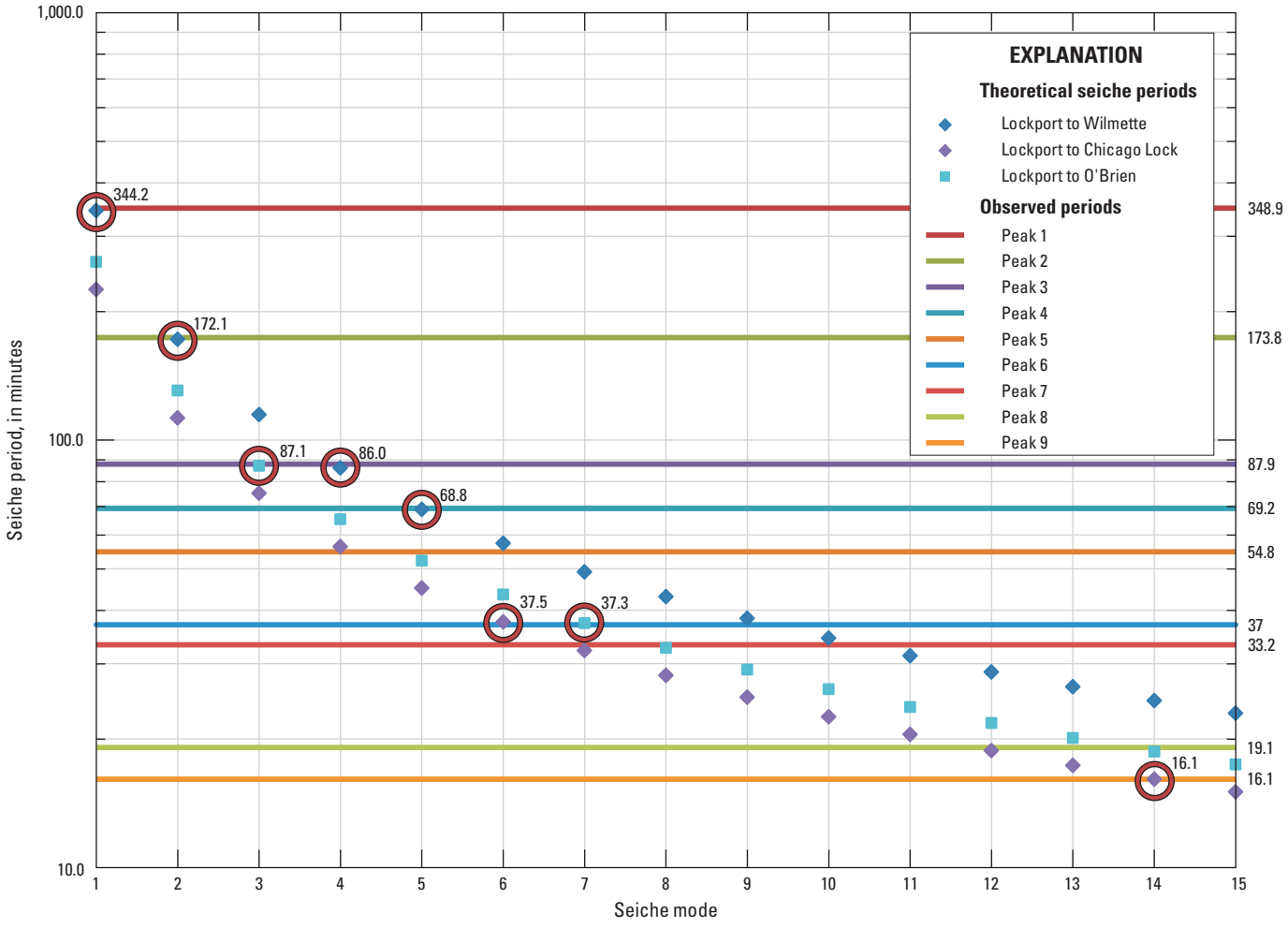

Figure 13. Seiche periods for the Chicago Area Waterways System (CAWS) compared to the observed dominant periods in the velocity data in the Chicago Sanitary and Ship Canal near Lemont, Illinois.

A total of 23 barges/tows traversed the measurement site in a period of 25 hours on May 20–21, 2008 (table 3). An additional 29 barge/tow passages were identified in up-looking ADCP data during June 18–24, 2009, and were used for comparison to the 2008 data. The 2008 up-looking ADCP data were collected by using high-resolution water mode 11, which is subject to data loss in turbulence and high-velocity flows. Therefore, barge/tow passages resulted in significant data loss in which all or nearly all velocity data from the up-looking ADCP were lost for an average of more than 4 minutes during each passage. However, the 2009 up-looking ADCP data were collected by using water mode 12, a more robust configuration that is more tolerant of turbulent flows. Very little data loss occurred during barge/tow passages with the up-looking ADCP in water mode 12.

Heading changes associated with compass errors owing to local magnetic field disturbance can be high during barge/tow passages. The heading changed over the range of 5 to 30 degrees with a median value of 10 degrees for the 23 barge/tow passages in the 2008 up-looking ADCP data (table 3). In nearly all cases, the errors caused a heading deviation that alternated about the true heading (that is, a positive bias followed by a negative bias or vice versa). Because the instrument is in a stable position on the bed (but not fixed to the bed), the heading was stable in the absence of barges/tows.

Table 3. Barge/tow passages in the Chicago Sanitary and Ship Canal near Lemont, Illinois, May 20, 2008 (14:00) to May 21, 2008 (15:00).

[CST, Central Standard Time; DS, downstream; US, upstream; --, median not applicable]

Barge number	Date	Time, CST	Disturbance time[1], in minutes	Direction of travel	Compass change, in degrees
1	5/20/08	15:36:15	7.28	DS	30
2	5/20/08	17:19:35	4.62	DS	18
3	5/20/08	19:09:23	5.38	DS	11
4	5/20/08	20:00:39	3.65	DS	12
5	5/20/08	20:06:40	7.47	US	15
6	5/20/08	20:37:56	6.85	US	21
7	5/20/08	23:07:42	2.08	US	10
8	5/21/08	00:01:21	6.03	DS	30
9	5/21/08	00:14:43	2.37	DS	10
10	5/21/08	00:34:23	5.87	US	20
11	5/21/08	01:10:17	2.68	DS	10
12	5/21/08	02:06:28	2.40	US	8
13	5/21/08	05:49:08	4.62	DS	8
14	5/21/08	06:23:26	6.02	US	10
15	5/21/08	07:47:15	1.75	DS	12
16	5/21/08	08:31:11	4.28	DS	10
17	5/21/08	09:20:52	7.30	US	10
18	5/21/08	10:06:35	4.43	DS	9
19	5/21/08	10:18:11	2.53	US	30
20	5/21/08	10:52:19	2.52	DS	8
21	5/21/08	13:21:56	2.37	DS	5
22	5/21/08	14:13:03	3.32	US	8
23	5/21/08	14:49:33	4.12	DS	9
Median	--	--	4.28	--	10.0

[1]Disturbance time denotes the time the flow was disturbed leading to significant loss of data from the 600-kHz Rio Grande acoustic Doppler current profiler with water mode 11.

The 2009 up-looking ADCP data had erroneous compass readings owing to a malfunctioning heading, pitch, and roll sensor, so it could not be used for comparison. The compass errors caused by barges may be problematic if the up-looking ADCP is ever used as an index velocity meter at the site. Index velocity computations require one to use the compass to determine instrument orientation (or use an instrument with no compass and a known, fixed orientation) so that the streamwise velocity can be determined. Nevertheless, these disturbances are short and well defined and may be useful as a flag or marker for data filtering. Compass deviations may also be a useful tool for counting the frequency of barge passages should that ever be required.

The barge/tow passages observed in May 2008 caused regular data loss in path 1 of the AVM but no data loss in paths 2 and 3. AVM data were analyzed for the periods of barge/tow passages identified from the up-looking ADCP data, and the analysis revealed that path 1 of the AVM regularly lost 14 to 28 minutes of data after a barge/tow passage, resulting in between 20 to 30 minutes of invalid data when averaged over 10-minute intervals. AVM paths 2 and 3 showed no data loss for the same barge/tow passages, indicating the disturbance is likely owing to blocking of AVM path 1 by fully loaded barges (9 ft draft) and air entrainment by the tow propellers and is confined to the near-surface layer. In general, for a median flow velocity of 0.75 ft/s, a 0.1- to 0.3-ft/s (13- to 40-percent) decrease in the flow velocity over all paths was associated with downstream-bound barges/tows, whereas a 0.2- to 0.5-ft/s (27- to 67-percent) increase in flow velocity accompanied upstream-bound barges/tows. Impacts of the barges/tows likely vary substantially with the size, loading, and speed of the barges.

The H-ADCP showed little to no data loss from 29 barge/tow passages in June 2009. Data from the June 2009 up-looking ADCP deployment were used in place of the May 2008 data because of a contamination of the H-ADCP data during the May 20–21, 2008, study (data were invalid because of human error in programming the instrument). Of the 29 barge/tow passages during the analyzed period, only 7 passages caused any loss of data in the H-ADCP, and the data loss was minimal. In general, only one cell (but up to three cells) of the H-ADCP were lost in response to the barge/tow passages. Data were lost in these cells for only 2 to 3 minutes after each passage. Fifteen of the passages have an associated change in measured velocity (taken as the mean of the H-ADCP cells), with changes ranging from approximately 0.2 to 0.5 ft/s (12 to 31 percent) for a mean velocity of 1.62 ft/s. Although the flow rate for this period was higher than for the May 20–21, 2008, data, the flow disturbances are similar in magnitude. The sustained flow velocity reached 3.7 ft/s for a 28-hour period during June 19 and 20, 2009, and although only one barge passed during this period, a velocity increase of 0.1 ft/s (2.6 percent) was observed during the passage. Therefore, although barge/tow passages may not create a large loss of H-ADCP data, they introduce uncertainty in the computed discharge at the site by modifying the velocity field for all flow rates observed at the site, resulting in errors or bias in the index velocity measurements. However, temporal averaging of the computed discharge at the daily, monthly, and annual time scales can substantially lessen any influence on the computed discharge from navigation.

Flow Variability Owing to Lockages

A significant source of variability in the flow in the CSSC near Lemont, Ill., is lockages at Lockport Lock, 11.5 mi downstream. Lockport Lock and Dam has an average 39.5-ft head difference across the structure and requires a large volume of water (approximately 2.6 million cubic feet) to fill the lock (U.S. Army Corps of Engineers,1986). Each time the lock is filled, the flow in the canal increases and a flood wave propagates upstream. Based on shallow-water wave theory, the rate of propagation of this wave upstream, or wave celerity, is approximately 23 ±3 ft/s after accounting for frictional effects (assuming a 20-percent decrease in wave celerity owing to friction; Geyer and Chant, 2006). Therefore, flood waves generated by the lock should affect the gage near Lemont approximately 40 to 51 minutes after the start of the filling of the lock chamber (for a mean channel depth of 25 ft).

To examine this source of variability, the data from the up-looking ADCP and the AVM were utilized for the period of May 20 and 21, 2008. During this 25-hour period, a total of eight vessels locked through at Lockport, with two of the vessels requiring two lockages to transit the lock because of their large size (table 4). Table 4 also lists the status of the lock chamber during filling because the rate at which it is filled is increased significantly when the chamber is empty (Pat Wharry, Lockport Lock Master, oral commun., 2010). By use of the up-looking ADCP and AVM data, velocity "pulses" associated with lockages were identified in the records and are listed in table 5, along with their general characteristics.

Increased velocity pulses near Lemont owing to lockages at Lockport Lock have a duration of about 33 minutes and an average midchannel velocity of about 1.1 ft/s for the time period analyzed (table 5). The time- and depth-averaged midchannel flow velocity based on the data from the up-looking ADCP for this period (May 20–21, 2008) was 0.55 ft/s; increases in velocity above the average velocity ranged from 0.6 to 0.7 ft/s (109 percent to 127 percent) for pulses generated by filling an occupied lock chamber to 0.7 to 0.8 ft/s (127 percent to 145 percent) for filling an empty lock chamber at Lockport Lock. The three paths of the AVM show a similar response to the up-looking ADCP, with about a 0.1-ft/s smaller peak pulse velocity (likely owing to spatial and temporal averaging of the data). The 33-minute average pulse duration is consistent with the time it takes to fill the lock under normal operating conditions (about 30 minutes for an occupied lock chamber) and is close to the 37-minute period observed in the AVM and H-ADCP data (table 2, peak 6).

Table 4. Lockages recorded at Lockport Lock on the Chicago Sanitary and Ship Canal, near Lemont, Illinois, May 20, 2008 (14:00), to May 21, 2008 (15:00).

[Data provided by the U.S. Army Corp of Engineers Rock Island District; CST, Central Standard Time; --, median not applicable]

Lockage number	Arrival time, CST	Lockage start time, CST	Lockage end time, CST	Lockage duration, in minutes	Travel direction	Cuts[1]	Chamber status during fill	Chamber filled during lockage?
1	5/20/08 14:50	5/20/08 14:50	5/20/08 16:20	90	Upstream	1	Occupied	Yes
2	5/20/08 14:39	5/20/08 16:20	5/20/08 17:29	69	Downstream	1	Occupied	No
3	5/20/08 18:53	5/20/08 18:53	5/20/08 19:52	59	Downstream	1	Empty	Yes
4	5/20/08 20:39	5/20/08 20:39	5/21/08 00:28	229	Upstream	2	Occupied	Yes (×2)
5	5/20/08 21:20	5/21/08 00:47	5/21/08 01:46	59	Upstream	1	Occupied	Yes
6	5/21/08 04:06	5/21/08 04:06	5/21/08 07:11	185	Upstream	2	Occupied	Yes (×2)
7	5/21/08 10:06	5/21/08 10:06	5/21/08 10:39	33	Downstream	1	Occupied	No
8	5/21/08 12:03	5/21/08 12:03	5/21/08 12:30	27	Downstream	1	Empty	Yes
9	5/21/08 13:44	5/21/08 13:44	5/21/08 14:15	31	Upstream	1	Occupied	Yes
10	5/21/08 14:25	5/21/08 14:25	5/21/08 17:31	186	Upstream	2	Occupied	Yes
Median	--	--	--	64	--	--	--	--

[1] "Cuts" denotes the number of lockages required to lock through a raft of barges (that is, two cuts means the load was split into two to pass through the lock).

Table 5. Velocity pulse characteristics recorded in the Chicago Sanitary and Ship Canal near Lemont, Illinois, associated with lockages at Lockport Lock, May 20, 2008 (14:00), to May 21, 2008 (15:00).

[CST, Central Standard Time; ft/s, foot per second; NA, not applicable]

Pulse number	Pulse start, CST	Pulse end, CST	Pulse duration, in minutes	Maximum pulse velocity, in ft/s	Associated lockage number	Pulse traveltime, in minutes	Lock loading[1] included?	Adjusted pulse traveltime,[2] in minutes	Comments
1	5/20/08 16:13	5/20/08 16:44	31.4	1.09	1	83.4	Yes	65.4	NA
2	5/20/08 19:37	5/20/08 20:00	23.0	1.30	3	44.8	No	44.8	NA
3	5/20/08 22:01	5/20/08 22:48	47.2	1.18	4	82.8	Yes	64.8	NA
4	5/20/08 23:21	5/20/08 23:55	33.9	.86	4	NA	NA	NA	NA
5	5/21/08 02:01	5/21/08 02:31	30.2	.85	5	74.3	Yes	56.3	NA
6	5/21/08 05:17	5/21/08 05:51	33.9	.92	6	71.3	Yes	53.3	NA
7	5/21/08 06:37	5/21/08 07:42	65.3	1.52	6	NA	NA	NA	NA
8	5/21/08 12:25	5/21/08 12:58	32.7	1.52	8	22.5	No	22.5	Lock pre-filled?
Median	NA	NA	33.3	1.1	NA	NA	NA	NA	NA

[1]Specifies whether the traveltime estimate includes the time to load the lock and close the gates.

[2]Adjusted traveltime removes 18 minutes from the traveltime estimate to account for lock loading (Pat Wharry, U.S. Army Corps of Engineers, oral commun., 2010).

The pulse traveltime from Lockport to Lemont is consistent with shallow-water wave theory. The traveltime to reach Lemont for a lock pulse generated by filling an unoccupied lock chamber at Lockport is approximately 45 minutes (table 5, pulse 2), well within the range predicted by shallow-water wave theory. Lockage number 7 was not used in this analysis because it appears that the lock was prefilled prior to the arrival time of the vessel (the start-of-lockage time appears to be stamped after the fill began, as supported by the very short pulse traveltime). For the case of a pulse generated by the filling of an occupied lock chamber, the start-of-lockage time is assigned when a vessel is permitted to enter the lock, and the filling of the lock starts after the vessel is secure in the lock and the gates are closed. The typical time required for this process is 15–20 minutes (Pat Wharry, Lockport Lock Master, oral commun., 2010). Therefore, the pulse traveltimes for these lockages were adjusted by the 18 minutes to remove the time prior to the start of lock filling. The adjusted pulse traveltimes for a pulse generated by filling an occupied lock range from 53 to 65 minutes, with a mean of 60 minutes, and are slightly longer than that predicted by shallow-water wave theory. These differences likely are owing to a combination of uncertainty about the exact time the lock began to fill and possibly a deviation from shallow-water wave theory.

Reverse Flows

The 1-minute H-ADCP data and 2-minute AVM data for the period November 2006–January 2010 were averaged over 10-minute periods, and reverse flows during each 10-minute observation were identified in each record. Table 6 shows the results of this comparison, including the percentage of observations with reverse flow in all cells/paths and in each individual cell/path, the median and maximum negative velocities observed during reversals, and the maximum period of sustained reverse flow.

Flow reversals occur in the CSSC near Lemont, Ill., but they only occur a very small percentage of the time. Data indicate that full channel flow reversals occur less than 0.1 percent of the time near Lemont (table 6). However, partial flow reversals (reversal flow in part of the cross section) occur more frequently. With the exception of the left bank of the canal, partial flow reversals generally occur between 0.13 percent and 0.48 percent of the time. Flow reversals on the left bank occurred 1.4 percent of the time during the observation period.

Table 6. Flow-reversal observations in the Chicago Sanitary and Ship Canal near Lemont, Illinois, November 2006–January 2010.

[Based on 10-minute averaged velocity data; ft/s, foot per second; AVM, acoustic velocity meter; H-ADCP, horizontal acoustic Doppler current profiler]

Instrument	Path/cell	Percent of observations with reverse flow	Median velocity during reversals, in ft/s	Maximum negative velocity during reversals, in ft/s	Maximum period of flow reversal, in minutes
AVM	All	0.07	−0.04	−0.24	80
	1	.13	−.04	−.24	160
	2	.23	−.04	−.22	90
	3	.32	−.03	−.25	160
H-ADCP	All	.08	−.04	−.56	70
	1	.46	−.05	−.57	120
	2	.41	−.05	−.51	150
	3	.39	−.05	−.50	150
	4	.41	−.05	−.45	170
	5	.44	−.05	−.67	180
	6	.42	−.04	−.52	180
	7	.48	−.04	−.84	110
	8	.66	−.02	−.64	190
	9	1.4	−.01	−.33	200

Flow reversals in the CSSC near Lemont, Ill., occur more regularly near the streambed and near the left bank. Table 6 shows that the AVM records indicate almost 3 times the number of flow reversals in path 3 (nearest the bed) than in path 1 (nearest the surface). It is important to note that partial flow reversals near the bed may be missed in index velocity measurements with the H-ADCP because of the lack of near-bed velocity measurements. However, given their relatively low occurrence rate and low magnitudes, it is unlikely that missed near-bed partial flow reversals will lead to large errors in computed discharge. Table 6 also shows that the H-ADCP records indicate more than 3 times the flow reversals in cell 9 (nearest the left bank) than in cell 1 (nearest the right bank). Both cells 8 and 9 indicate that flow reversals are more common on the left bank of the channel.

Flow reversals near Lemont are generally small in magnitude. Median values of flow velocity range from −0.01 to −0.05 ft/s; however, individual 10-minute averages range from −0.22 to −0.84 ft/s. It should be noted that the maximum reverse flow velocity observed by the H-ADCP is more than twice that observed by the AVM for path 2. This difference may be owing to the higher noise levels and smaller sampling volume in the H-ADCP measurements compared to the AVM measurements.

The maximum values of reverse flow generally occurred in periods of sustained reverse flow, thus allowing periods of upstream transport. Reverse-flow periods ranged from 90 to 200 minutes in individual cells/paths, whereas full-cross-section reversals occurred for periods of 70 to 80 minutes. Such reversals could have implications for transport of contaminants and biological constituents upstream.

Stratification and Salinity Variation

Stratification of the water column can lead to density-driven flows in the CAWS (Jackson and others, 2008). Such stratified flows in the CAWS arise primarily from differences in the temperature and salinity (owing to road-salt runoff) over the depth. In a branched system such as the CAWS, variable flow depths and numerous inflows can cause significant differences in density between branches, thus leading to the formation of density currents (Jackson and others, 2008). Index velocity measurements can be susceptible to errors in stratified flows and flows with variable salinity. Changes in salinity cause a change in the speed of sound, a fundamental property used by all acoustic meters. Stratified conditions can significantly change the velocity distribution in the water column by generating complex or bidirectional flows, leading to large errors in index velocity measurements (Jackson and others, 2008). In addition, ray bending can occur as sound emitted by the acoustic instrument passes through a strong stratification, altering its direction of travel and leading to contamination or loss of data. Salinity variations are common in tidal locations and are accounted for by using a mean salinity for speed-of-sound computations (Levesque and Oberg, in press). In general, ADCPs must account for salinity to accurately measure water velocities. The AVM is a traveltime meter and uses the difference in traveltime for a sound pulse moving with the current and against the current. In general, an AVM is not susceptible to errors caused by variable salinity provided the speed of sound does not change significantly between the two pulses.

Data from a thermistor and conductivity string deployed by the USGS in the CSSC near Lemont from March 2009 to May 2010 reveal that the canal does stratify in this reach. The primary contributor to the stratification is temperature, the largest temperature stratification occurring between September and April during sustained periods of low flow. During these months, the temperature difference between the streambed and the water surface can be greater than 5°C and is likely a result of wastewater inflows and discharges of cooling water from power generation plants in the system upstream. The Calumet Sag Channel upstream of Lemont may be also causing periods of stratified flow at Lemont (upstream-propagating density currents were documented by the authors just upstream of the confluence of the Calumet Sag Channel and the CSSC in December 2010). During the rest of the year, the temperature difference in the water column is generally less than 0.2°C. By comparison, the flow shows little overall stratification with respect to salinity, with typical changes over the water column of approximately 0.025 ppt for most of the year. However, the overall salinity does increase dramatically during the winter months in this system, with salinities approaching 2 ppt (and specific conductance values greater than 3,500 µS/cm) following winter storm events, a consequence of road-salt runoff (Jackson and others, 2008). In general, high-flow events break the stratification, and the entire water column has a uniform temperature and salinity for a period following high flows.

To estimate the potential error caused by not accounting for salinity variations in index velocity measurements in the CSSC near Lemont, BM-ADCP discharge measurements collected during a period of elevated salinity were recomputed to account for a salinity of 1 ppt and 2 ppt rather than zero. For the two measurements analyzed, this resulted in an increase in discharge of 0.23 and 0.47 percent for the 1 ppt and 2 ppt increase in salinity, respectively. In addition, the average velocities for each measurement with and without the salinity correction were compared and found to have a mean increase of 0.1 to 0.5 percent when accounting for a salinity of 1 ppt.

Therefore, owing to unaccounted-for changes in salinity in the CSSC, the H-ADCP can be expected to be biased low by less than about 0.5 percent during periods of high salinity, which typically occur in the winter following storm events (Jackson and others, 2008). The discharge measured by the AVM should not be affected by the salinity change, owing to the principles of operation of the AVM. A comparison of 480 daily mean discharges between March 15, 2009, and December 31, 2010, computed by using the AVM (not affected by salinity variation) and H-ADCP (affected by salinity variation) found that the difference in computed discharge ($Q_{H\text{-}ADCP} - Q_{AVM}$) was weakly correlated ($r = 0.31$) with specific conductance measured just below the depth of the H-ADCP (approximately 560.8 ft NAVD 88). This weak, positive correlation is opposite in sign to that predicted by correction of discharge measurements for salinity increases; therefore, it is likely that this weak correlation is owing to seasonal changes in canal operation (discretionary diversion of Lake Michigan water ceases during the winter) rather than variations in specific conductance.

Velocity Profiles

Vertical

Vertical velocity profiles in the CSSC near Lemont, Ill., were analyzed for three different temporal scales: 15-minute average profiles from a BM-ADCP, a 26-hour average profile obtained from an up-looking ADCP, and long-term average profiles from approximately 4 years of data from the AVM. Investigating the vertical flow profile at this range of scales allows one to look past effects from turbulence and complex flow structure and effects from the highly variable flows seen in the CSSC near Lemont, Ill.

For this analysis, near-instantaneous flow profiles were obtained near the center point of each cell of the H-ADCP by using a BM-ADCP on May 20, 2008. This experiment yielded 15-minute, temporally averaged flow profiles at nine points across the channel in the CSSC near Lemont. In addition, data from the up-looking ADCP deployed for a 26-hour period during May 20–21, 2008, was averaged and used to define a short-term, temporally averaged vertical velocity profile. To define a long-term, temporally averaged flow profile, velocity data in all three paths of the AVM near Lemont were averaged for the period December 2005 to February 2010. In addition to averaging all the observed values for each path, the velocity data were grouped into three categories based on the path 2 velocity (< 1.0 ft/s, 1.0 to 3.0 ft/s, and > 3.0 ft/s) and averaged within each velocity range (grouping approximately follows the primary ranges of velocity observed at the site as, shown in figs. 7 and 8). In all cases, the vertical flow profiles were compared to the logarithmic and generalized power law models for velocity distribution in open channels (Chen, 1991). Both the one-sixth power law and generalized, variable exponent power law were compared to the observed data (table 7). The one-sixth power law is equivalent to Manning's equation for mean velocity in a uniform flow (Chen, 1991).

Near-instantaneous vertical velocity profiles can vary significantly across the channel near Lemont. Figure 14 shows the 15-minute average velocity profiles obtained with a BM-ADCP on a tag line. In spite of averaging nearly 1,500 individual velocity profiles at each location, profiles at many sections show evidence of turbulence and complex flows and fit poorly with either the log law or the power law. These poor fits lead to great variability in the shear velocity, u^*, and roughness length, z_0 (table 7). The flow approaches a more logarithmic profile near the center of the channel (cells 4 and 5) and the left bank (cells 8 and 9). Much of the flow variability can be attributed to unsteadiness and barge traffic. During these measurements, a flood wave passed through the CSSC at Lemont, causing the discharge to nearly triple (1,225 to 3,490 ft^3/s) and then drop again to 1,500 ft^3/s. Smaller fluctuations of 500 to 1,000 ft^3/s were superimposed on this flood wave. The AVM path velocities showed a nonuniform response to this flood wave. Path 3 of the AVM (nearest the bed) saw a fourfold increase in velocity during the flood wave, whereas path 1 saw a twofold increase in velocity. In addition, two barges passed the site during these measurements, and data collection was suspended for a period before and after barge passage. However, the effect of the downstream-bound barges can be seen on the flow profiles in cells 1, 2, 6, and 7 (a barge passed the site after measurements in cell 1 and cell 6). Deceleration also is evident at the top of each of the measured profiles. Although winds from the northwest at 10–15 mi/h were observed in the area during the measurements, field notes recorded a observation of "light upstream wind" during the measurements. Flow disturbance owing to the ADCP and manned boat can cause flow deceleration near the surface. Mueller and others (2007) showed that flow disturbance from just the ADCP can extend beyond the blanking distance of the instrument and contaminate velocity data closest to the unit. The deceleration seen in the measured profiles near the surface is believed to be primarily owing to a combination of wind and disturbance from the manned boat.

Table 7. Vertical velocity profile properties for a range of flow conditions in the Chicago Sanitary and Ship Canal near Lemont and Romeoville, Illinois.

[ft/s, foor per second; u, streamwise velocity, in ft/s; u^*, shear velocity; κ, Von Karman constant; z, height above the bed, in feet (ft); z_0, roughness length; R^2, coefficient of determination; a, power law coefficient; n, power law exponent; C_p, Chen product $C_p = \kappa^* a^* n^* e$; e, base of natural logarithms; "Position" is the location of the measured profile in the channel; BM-ADCP, boat mounted acoustic Doppler current profiler; AVM, acoustic velocity meter; --, not applicable; <, less than; >, greater than]

Instrument	Position	Mean velocity, in ft/s	Log law, $u/u^* = 1/\kappa \ln(z/z_0)$			Power law, $u/u^* = a(z/z_0)^n$				Power law, $u/u^* = a(z/z_0)^{1/6}$			
			u^*, in ft/s	z_0, in ft	R^2	a	n	R^2	C_P	a	n	R^2	C_P
BM-ADCP[1]	Cell 1	0.42	0.099	1.828	0.876	1.32	0.634	0.857	0.933	3.25	0.167	0.426	0.603
	Cell 2	.45	.060	.507	.939	2.44	.358	.934	.973	4.49	.167	.691	.833
	Cell 3	.36	.029	.069	.875	4.29	.207	.859	.990	5.29	.167	.830	.982
	Cell 4	.80	.062	.053	.973	4.51	.197	.966	.991	5.32	.167	.945	.989
	Cell 5	.69	.099	.623	.963	2.18	.397	.992	.963	4.36	.167	.687	.809
	Cell 6	.57	.100	1.071	.919	1.62	.519	.982	.935	3.89	.167	.569	.723
	Cell 7	.43	.027	.015	.914	5.85	.153	.885	.995	5.32	.167	.879	.989
	Cell 8	.47	.036	.050	.952	4.71	.189	.934	.994	5.34	.167	.922	.991
	Cell 9	.38	.042	.265	.983	3.12	.283	.967	.984	4.89	.167	.818	.908
Up-looking ADCP	Center	.54	.047	.097	.991	3.96	.225	.997	.992	5.22	.167	.935	.970
AVM	--	.75	.053	.040	.994	5.09	.176	.997	.998	5.37	.167	.994	.998
		< 1.0	.047	.058	.995	4.76	.188	.998	.998	5.35	.167	.985	.993
		1 to 3	.064	.004	.994	7.29	.123	.996	.999	5.09	.167	.873	.945
		> 3.0	.199	.006	.994	6.80	.132	.991	.999	5.21	.167	.923	.968
Romeoville ADCP[2]	Center	.95	.066	.030	--	4.88	.182	--	--	5.35	.167	--	--
		2.23	.151	.025	--	5.17	.173	--	--	5.35	.167	--	--

[1]Velocity and discharge were highly unsteady during measurements.

[2]From González and others (1996).

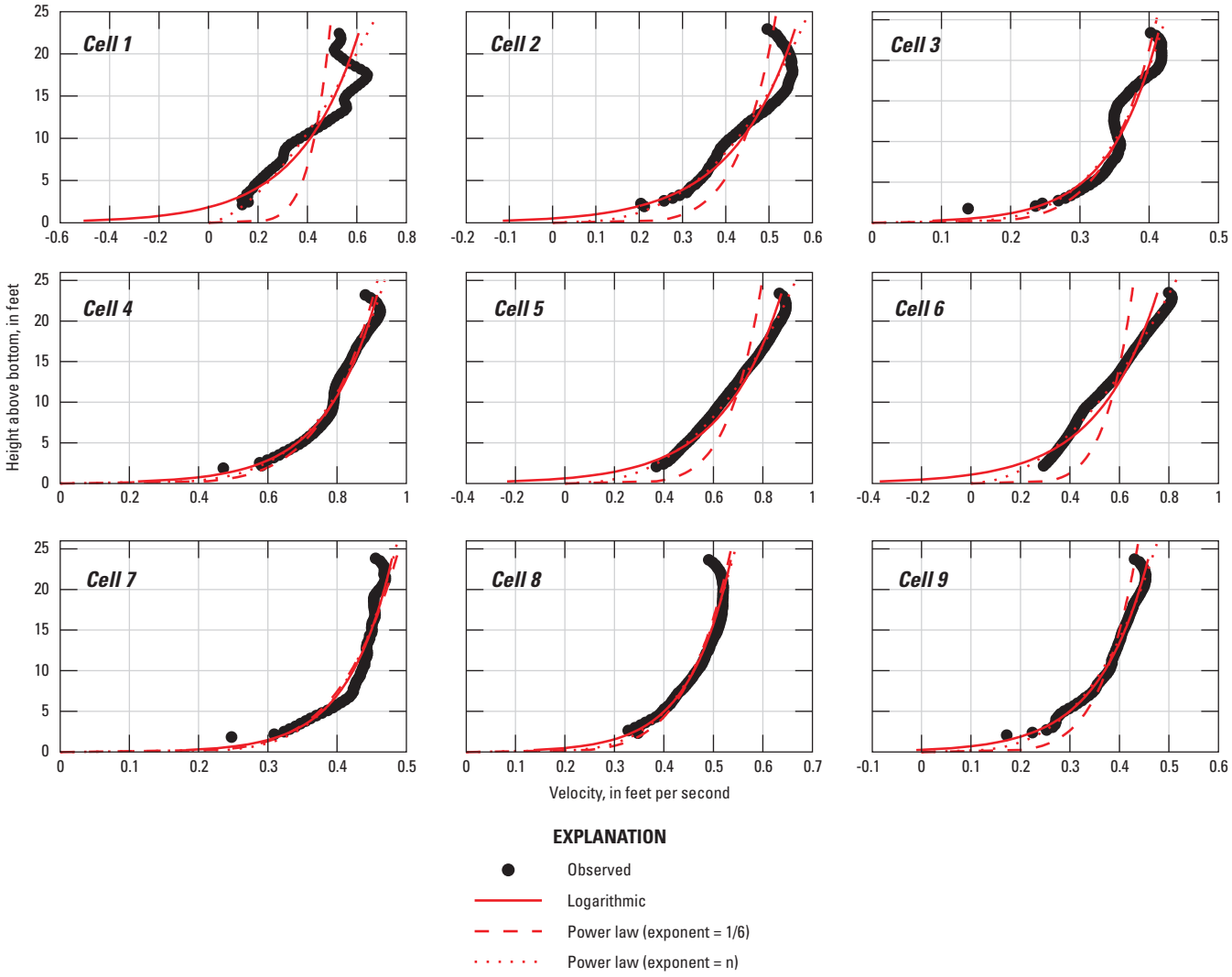

Figure 14. Fifteen-minute average vertical velocity profiles measured near the center of each of the nine cells of the horizontal acoustic Doppler current profiler (H-ADCP) by using a boat-mounted acoustic Doppler current profiler (BM-ADCP) in the Chicago Sanitary and Ship Canal near Lemont, Illinois, May 20, 2008.

The short-term average flow profile measured by the up-looking ADCP in the CSSC near Lemont, Ill., during the 26-hour deployment in 2008 fits a logarithmic profile with slight deviation near the boundaries (fig. 15). The fitting parameters, including the shear velocity and roughness length, are given in table 7. The roughness length, z_0, is considerably larger than that measured by a BM-ADCP in 1994 and 1995 in the CSSC at Romeoville, Ill., by Gonzales and others (1996). It is also larger than values obtained from fitting 15-minute averaged data in cells 4 and 8 (two of the best log law fits). The increase in roughness length is likely owing to a improper fit of the near-bed data by the log law (fitting only the lower 10 percent of the data results in $u^* = 0.032$ ft/s and $z_0 = 0.017$ ft). Like the May 20, 2008, BM-ADCP data, this 26-hour up-looking ADCP dataset includes highly unsteady flow. During the measurement period, seven flood waves passed through the CSSC at Lemont with at least 2,000 ft^3/s increase in flow rate. One flood pulse consisted of a 4,500 ft^3/s increase (250 ft^3/s to 4,710 ft^3/s) in just over 3 hours. Although discharge averaged approximately 2,000 ft^3/s during the measurement period, the range of discharges observed ranged from −50 to 4,710 ft^3/s. Although much of the variability in shear velocity and roughness length is likely owing to unsteadiness, a combination of the increased bed roughness created by sloughed banks near Lemont and the drag created by the up-looking ADCP and mount sitting on the bottom could also lead to an increased roughness length. An ADCP without the up-looking mount is capable of producing a flow disturbance out to 1.6 ft from the instrument under the range of flows observed during this deployment (Mueller and others, 2007). Unlike the profiles measured at Romeoville, Ill., which fit the one-sixth power law, the one-sixth power law fails to fit the profile from the up-looking ADCP near Lemont, Ill. The profile near Lemont is closer to a one-fifth (or even one-fourth) power law based on 26 hours of velocity data.

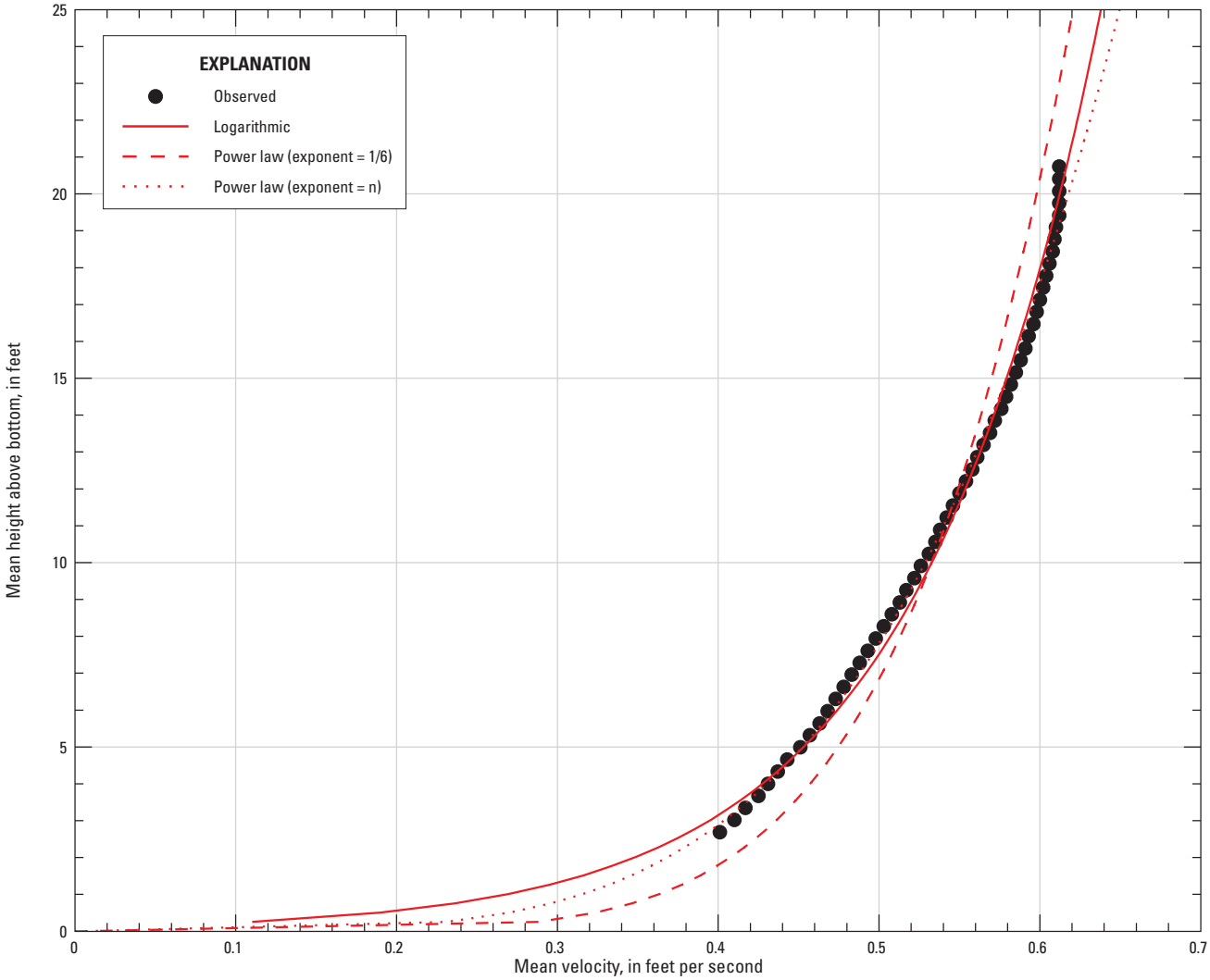

Figure 15. Twenty-six-hour average vertical velocity profile measured by using an up-looking, bottom-mounted acoustic Doppler current profiler in the Chicago Sanitary and Ship Canal near Lemont, Illinois, May 20–21, 2008.

Although instantaneous and short-term averaged vertical velocity profiles may deviate from a logarithmic profile (as indicated by boat-mounted and up-looking ADCP data), the long-term time-averaged data indicate the vertical velocity profile in the CSSC near Lemont, Ill., is a logarithmic distribution under a range of flow conditions (fig. 16). In addition, figure 16 shows the averaged data fit with a one-sixth power law primarily for low velocities (< 1 ft/s). Higher flow velocities exhibit a deviation for the one-sixth power law yet continue to fit a logarithmic distribution. On average, power law exponents approach a one-eighth power law at velocities greater than 1.0 ft/s, though only three points are fitted in the profile and there are far fewer observations at high flows.

Transverse

Although the multipath AVM near Lemont can describe the vertical velocity distribution to some extent, it cannot yield any information about the transverse velocity distribution. However, the multi-cell configuration of the H-ADCP can describe the transverse velocity profile near middepth in the CSSC near Lemont, Ill., for a wide range of flow conditions. Data from the H-ADCP for the period November 2006–January 2010 were used to define the average transverse velocity profile for a range of flows. The data were grouped according to index velocity range (that is, nine-cell average) and temporally averaged within each respective cell for the entire record. In addition, ADCP data collected from a boat-mounted ADCP during discharge measurements with GPS data were extracted, mapped to the fixed measurement cross section, depth averaged, and spatially averaged within each of the nine cells defined by the configuration of the H-ADCP. To ensure accurate positioning of the data within the cross section, those measurements collected at nearby cross sections and those without GPS data were omitted from this analysis.

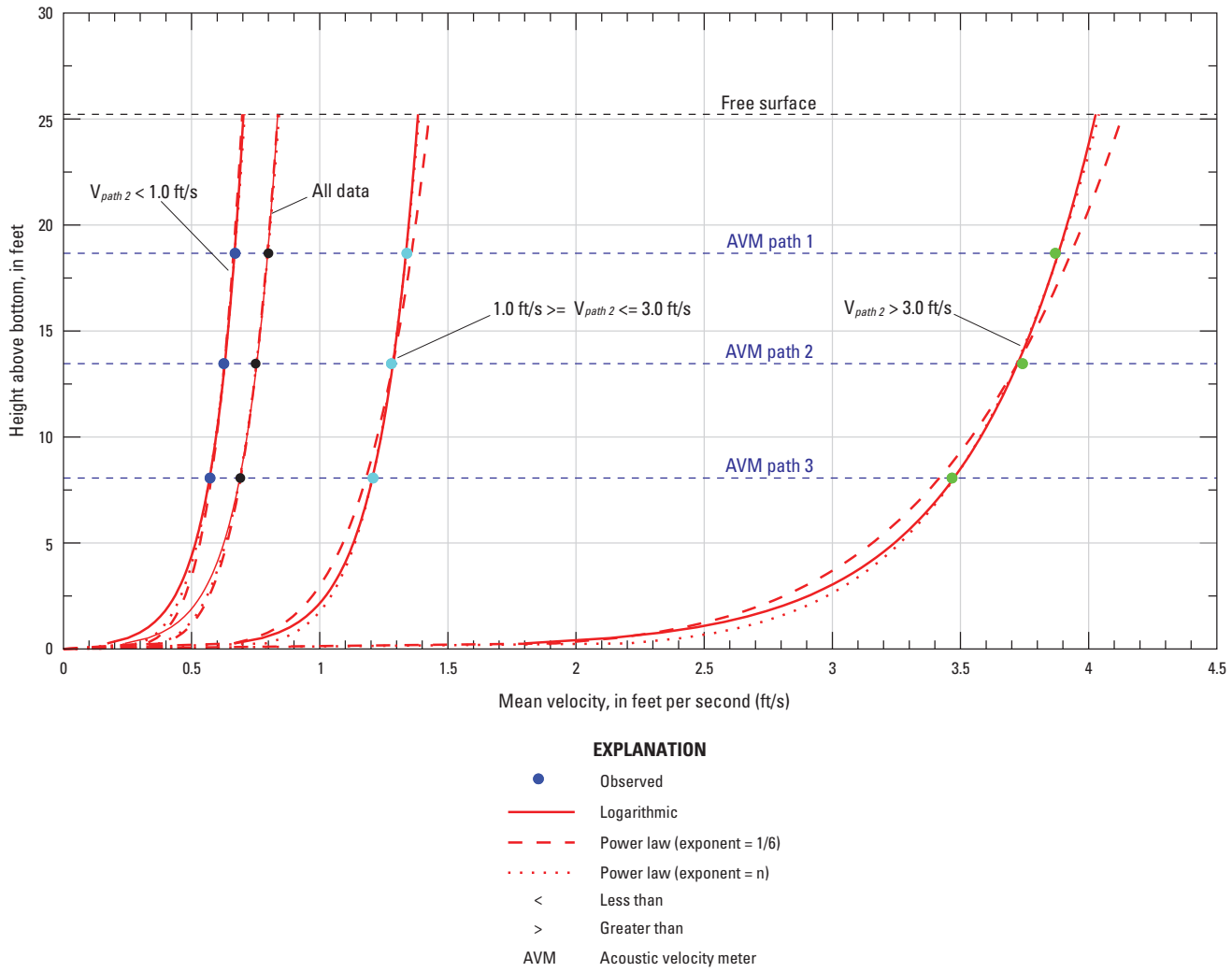

Figure 16. Four-year average vertical velocity profiles measured by the three paths of the acoustic velocity meter (AVM) in the Chicago Sanitary and Ship Canal near Lemont, Illinois, December 2005 to February 2010. Data are grouped according to path 2 velocity range, and line types are as defined in figure 15.

Of the 61 discharge measurements collected near Lemont, Ill., before April 2010, 29 measurements met the above criteria and were used in this analysis. For this analysis, the velocity data have been normalized by the maximum velocity in the cross section, allowing a collapse of the wide range of flow magnitudes near Lemont.

In general, the H-ADCP data show that the transverse flow distribution near Lemont is skewed to the right bank (looking downstream) for flows less than 3.0 ft/s and skewed to the left bank for flows greater than 3.0 ft/s (fig. 17). As the flow velocity increases in the cross section near Lemont, the velocity on the left bank increases by as much as 60 percent, whereas the flow velocity on the right bank decreases by about 3 percent. This skew to the left bank at high velocities is likely related to the channel curvature near Lemont, which would generate higher flows to the outside of the bend. In general, the maximum velocities occur in cells 3 and 4 at low flows and cells 5 and 6 at high flows.

The sharp change in the velocity in cell 9 immediately adjacent to the left bank deserves further discussion. Data from the H-ADCP show a 40-percent decrease in flow velocity between cell 8 and cell 9 and a deviation from the standard beta distribution fit for transverse velocity profiles (Seo and Baek, 2004). There are several possible reasons for this discontinuity. First, impingement of the acoustic beam on the far wall, the bed, or contamination by side-lobe interference could be creating a low bias in cell 9. However, the far edge of cell 9 is 12 ft from the left bank and is outside of the 10-ft side-lobe zone (6 percent of channel width). Cell 9 is also 9.0 ft from the bottom at the far bank, so beam impingement on the bottom is unlikely. Also, there is no evidence of abrupt signal attenuation in cell 9 during instrument beam checks. Although past beam check data do not support side-lobe interference from the bed or the water surface, it is possible that the interference is subtle and may not be recognized in the data. More rigorous analysis of the beam-check data will be required in the future at this site.

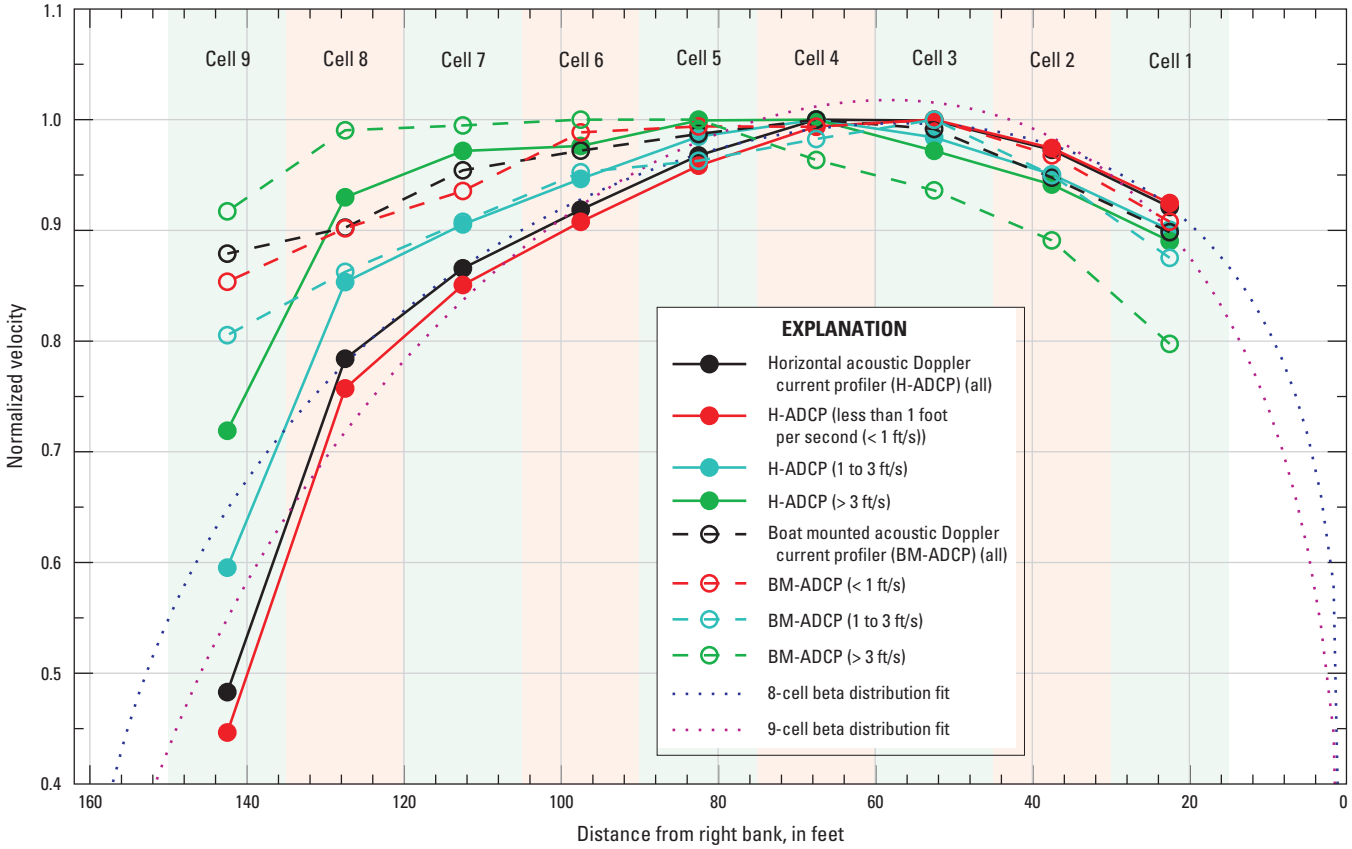

Figure 17. Transverse normalized velocity profiles in the Chicago Sanitary and Ship Canal near Lemont, Illinois, as measured by the horizontal acoustic Doppler current profiler (H-ADCP) and boat-mounted acoustic Doppler current profiler (BM-ADCP) for a range of flow velocities.

Another possible explanation for lower velocities in cell 9 is the proximity to the canal wall. Cell 9 is 3 ft closer to the boundary (12 ft) than cell 1, which is 15 ft from the right bank. The no-slip condition at the bank requires a sharp decrease in the velocity near the banks, and cell 9 may be showing an artifact of this flow deceleration. However, the 29 measurements made with a boat-mounted ADCP at the site do not show (on average) this flow deceleration in cell 9. A third explanation for the discontinuity would be the influence of the Calumet Sag Channel confluence upstream. Low flows from the Calumet Sag Channel, which joins the left bank of the CSSC 0.7 mi upstream of Lemont, could be hugging the left bank, generating a shear layer and causing a sharp decrease in flow velocity. Although time-averaged boat-mounted discharge measurements do not reflect this discontinuity, several individual measurements have shown a sharp 45- to 65-percent decrease in velocity near the left bank. The abrupt decrease in velocity is associated with an increase in backscatter, possibly indicating the presence of a second water mass made up of Calumet Sag Channel water hugging the left bank (aerial photos show the Calumet Sag Channel water is often more turbid than CSSC water, owing to shallower depth and input from numerous tributaries). Finally, located between the diverging beams of the H-ADCP is a mound on the bed near the left bank that is entirely within the width of cell 9 (see fig. 2). It is possible that this mound, which is 3.8 ft off the otherwise uniform bottom, could be causing a flow disturbance within the measurement volume of the H-ADCP cell 9 and causing the low bias. Nevertheless, the likely cause for this discontinuity in cell 9 is likely a combination of the above factors that manifest themselves under conditions that are not accurately captured in discharge measurements.

Comparison of Instrument Performance

This section presents comparisons of instrument performance with regard to index velocity measurements. This analysis includes a comparison of instrument reliability with a discussion of missing record, a comparison of velocity statistics including variance in the path and cell velocities, and a comparison of the most recent ratings curves developed for these instruments.

Instrument Reliability

The USGS streamgage on the CSSC near Lemont, Ill., must be accurate and reliable. Periods of missing data occur at all streamgages, but the importance of this gage for diversion accounting dictates that missing data must be minimized and measurement redundancy must be provided for. "Missing data" is defined as data that are lost because of an instrument malfunction or service outage (for example a power failure) or are marked invalid. "Invalid data" is defined as velocity data that are collected while the instrument is operational, but the data have been marked as invalid during internal instrument checks (for example, turbulence from a barge may cause correlations to fall below a predefined threshold set by the manufacturer). Data are considered valid if the instrument is functioning properly and velocity data have passed all internal instrument checks.

Since the installation of the gage near Lemont, the AVM has been the primary index velocity meter and the H-ADCP has been the backup. The remainder of this section examines the data records from these two instruments and compares their reliability for the period November 2006–December 2010. Velocity data (10-minute data) were used in this analysis. Missing data occur when either an invalid value (defined by each instrument for specific configuration settings) or no value is reported for a path/cell of the instrument during a sampling interval. Therefore, the percentage of missing data for each instrument includes both invalid velocity data and lost data from when the instrument was out of service. This is particularly important to note for the AVM, which was out of service from January 7, 2008, to May 20, 2008, because of severed cross-channel cables that had to be replaced by divers (requiring a service contract that delayed the repair); from September 7, 2009, to December 15, 2009, because of an equipment failure and unavailability of replacement parts; and from June 23, 2010, to July 9, 2010, because of a power-supply issue with the AVM. The only significant period of missing record for the H-ADCP was from July 12, 2007, to July 25, 2007, during an equipment malfunction.

The AVM has a substantially higher percentage of missing record compared to the H-ADCP over the same period from November 2006–December 2010 (table 8). During this period, the AVM returned no valid data on any path 16.7 percent of the time compared to 0.89 percent invalid data for the H-ADCP. The primary reason for this large difference is the time the AVM was out of service because of an instrument failure from severed cross-channel cables. If one considers only the time during which the instrument was operational, the percentage of missing data drops considerably. Table 8 lists the percentage of missing data by AVM path and H-ADCP cell.

Overall, during the time the instruments were operational, the AVM had invalid data on path 1 approximately 19.8 percent of the time, whereas it had invalid on paths 2 and 3 less than 0.03 percent of the time. This finding indicates that path 1 is highly susceptible to erroneous data, likely produced by barge/tow traffic, but that these disturbances do not invalidate velocities on paths 2 and 3. During a 26-hour period in May 2008, there were 23 barge/tow passages through the measurement reach, resulting in approximately 30 percent invalid data on path 1 (an average of 20 minutes lost per vessel). The AVM path 2 percentage of invalid data (during instrument operation) of 0.01 percent is very close to the average percentage of invalid data (during instrument operation) for all cells of the H-ADCP of 0.03 percent (found by omitting dates of instrument failure in July 2007). This finding indicates that the AVM path 2 and the H-ADCP located at the same elevation in the water column are equally reliable on average. With regard to individual path/cell reliability, the most reliable path of the AVM is path 2, and the least reliable is path 1. Cell 6 proved to be the most reliable for the H-ADCP, and cell 1 was the least reliable.

Table 8. Comparison of missing data by individual path/cell for the two index velocity meters in the Chicago Sanitary and Ship Canal near Lemont, Illinois, November 2006–December 2010.

[AVM, acoustic velocity meter; H-ADCP, horizontal acoustic Doppler current profiler]

Instrument	Path/cell	Percent missing (total)	Percent invalid (with 1 or more valid path/cell)	Percent lost (all paths/cells missing)
AVM	1	36.5	19.8	16.7
	2	16.8	.01	16.7
	3	16.8	.02	16.7
H-ADCP	1	.99	.10	.89
	2	.97	.08	.89
	3	.97	.08	.89
	4	.97	.08	.89
	5	.96	.07	.89
	6	.93	.04	.89
	7	.95	.05	.89
	8	.98	.09	.89
	9	.95	.06	.89

Analysis of the instrument records by number of valid paths for the AVM and cell for the H-ADCP reveals that the AVM reports valid data on all paths only 63.5 percent of the time compared to valid data for all cells of the H-ADCP 98.7 percent of the time (table 9). The primary reasons for this difference is the large period of missing data for the AVM during service outages and the contamination of path 1 by vessel traffic. The comparison also shows that loss of data on two paths of the AVM is rare (occurs only 0.03 percent of the time). Loss of one cell on the H-ADCP is most common (occurs 0.32 percent of the time), and the likelihood of missing more than one cell decreases with increasing number of cells lost (with the exception of all nine cells invalid). This result correlates well with the 6-day period in June 2009, where impacts of barge/tow passages on the H-ADCP were typically limited to contamination in only one cell. For the H-ADCP, it is relatively rare to have partially valid data. Generally, either all the cells are valid or invalid for a sampling period.

Table 9. Comparison of missing data by number of paths/cells for the two index velocity meters in the Chicago Sanitary and Ship Canal near Lemont, Illinois, November 2006–December 2010.

[AVM, acoustic velocity meter; H-ADCP, horizontal acoustic Doppler current profiler]

Instrument	Number of missing paths/cells	Percent of observations missing
AVM	0	63.5
	1	19.7
	2	.03
	3	16.7
H-ADCP	0	98.66
	1	.32
	2	.08
	3	.03
	4	.01
	5	.005
	6	.002
	7	.001
	8	.0
	9	.89

Velocity Statistics

The statistics of the observed velocity records for each path of the AVM and each cell of the H-ADCP can provide insight into instrument performance. For November 2006–January 2010, the velocity data (2-minute data for the AVM and 1-minute data for the H-ADCP) for each for the instruments were used to compute 10-minute averages. Basic statistics were then computed for each instrument record, and the results are given in table 10.

The minimum and maximum velocities observed for each instrument compare well, but there are subtle differences. The minimum velocities (all negative or upstream) recorded by the AVM are generally consistent across all three paths, with a slight increase in negative flow near the bed. However, the H-ADCP shows significant variability in minimum (upstream) velocities across the cross section. The highest upstream flows occur in cells 5, 7, and 8, indicating flow reversals are more pronounced toward the left bank (however, cell 9 shows the lowest negative flow). Averaging across all nine cells results in a mean minimum velocity of −0.21 ft/s which compares very well with the minimum velocity observed on path 2 of the AVM (−0.22 ft/s). The maximum observed velocities do not compare as well between instruments. The H-ADCP nine-cell average maximum velocity is almost 4 percent higher than the maximum velocity observed on path 2 of the AVM. The higher H-ADCP maximum velocity is likely owing to the fact that data near the banks are not measured with the H-ADCP (lower flows near the banks would lower the mean velocity). Finally, the highest velocities occur near the surface (as expected) and closer to the left bank at high flows, as previously discussed in the velocity profiles section.

The median observed velocities for each instrument show a skew in the flow to the right bank and a 10.1 percent higher median velocity for path 2 of the AVM compared to the H-ADCP. The bias of the flow to the right bank on average was discussed in the velocity profiles section and may be owing to influence from the confluence with the Calumet Sag Channel upstream and other factors. The 10.1-percent difference in median flow velocity for the two instruments at the same elevation in the water column is counterintuitive; one would expect that the H-ADCP would have a greater median velocity than AVM path 2 because the nine-cell average does not include data from unmeasured zones near the banks, where the velocity is lower. One possible explanation for the greater median flow velocity registered by the AVM is the reduced cross-sectional area in the AVM cross section compared to the H-ADCP cross section owing to a sloughed bank. Figure 2 shows the sloughed bank just downstream of the upstream notch in the canal wall on the right bank. By using bathymetry collected by the USGS and University of Illinois in 2010, cross sections were extracted at the upstream notch and halfway between the upstream and downstream notches. There is a 13.7 percent decrease in cross-sectional area within the AVM measurement volume between the notches. This reduction in flow area is capable of producing an increase in velocity magnitude in the AVM measurement volume that is proportional to the observed difference in the median velocities for the two instruments.

Table 10. Comparison of velocity statistics by individual path/cell for the two index velocity meters in the Chicago Sanitary and Ship Canal near Lemont, Illinois, November 2006–January 2010.

[ft/s, foot per second; AVM, acoustic velocity meter; H-ADCP, horizontal acoustic Doppler current profiler]

Instrument	Path/cell	Minimum observed velocity, in ft/s	Maximum observed velocity, in ft/s	Median observed velocity, in ft/s	Velocity variance[1], in (ft/s)^2
AVM	1	−0.24	5.06	0.80	0.0413
	2	−.22	4.81	.76	.0450
	3	−.25	4.47	.70	.0457
H-ADCP	1	−.57	4.56	.72	.1964
	2	−.51	4.85	.76	.1972
	3	−.50	5.10	.78	.2036
	4	−.45	5.19	.78	.2100
	5	−.67	5.42	.76	.2103
	6	−.52	5.59	.72	.2024
	7	−.84	5.54	.68	.1940
	8	−.64	5.17	.62	.1848
	9	−.33	4.16	.39	.1523
	9-cell average	−.21	5.00	.69	.1251

[1]Mean value of variance computed over 10-minute averaging intervals.

The mean variance in the 10-minute average velocity records is nearly 3 times higher for the nine-cell average of the H-ADCP than for path 2 of the AVM. This result implies that the H-ADCP has significantly more noise in the data than the AVM. Although the AVM has a larger sampling volume (about 45 percent, owing to the 44.5-degree angle of the paths across the channel) and longer unit value averaging (2 minutes) compared to the H-ADCP (1 minute), this increased spatial and temporal averaging is likely not enough to account for this difference in variance. Further comparison is difficult because the instruments' operation involves very different measurement techniques. The AVM uses a bulk flow measurement technique that is inherently less variable than the H-ADCP technique, in which bulk flows are reconstructed from velocities of individual particles in the water. Finally, the velocity variance is similar across all paths of the AVM and relatively uniform for all cells of the H-ADCP with the exception of cell 9 near the left bank (and to a lesser extent, cell 8). Cell 9 of the H-ADCP showed a 24 percent lower variance than the mean variance of the other eight cells, indicating that the velocity in cell 9 is less variable than that in the other cells. Instrument noise should be uniform across all the cells; however, in spite of the fact that the cell sizes are all equal, the 1.5-degree beam width results in an increase in sampling volume with distance from the meter. Theoretically, random errors should decrease proportional to $n_s^{-0.5}$, where n_s is the number of samples. If each particle in the measurement volume is considered a sample of the velocity, then the random error should decrease with distance from the meter because of the larger number of particles in the sampling volume. However, this explanation does not account for the distribution of velocity variance across the channel and the sharp decrease in variance in cell 9. Therefore, the decrease in variance in cell 9 (and to a lesser extent cell 8) may be owing to less turbulence in the flow. This latter explanation supports the hypothesis that cell 9 resides primarily in Calumet Sag Channel water, which may hug the left bank under typical flow conditions and which possess a lower turbulence intensity (and higher backscatter) than the main flow in the CSSC. This hypothesis could be tested through a targeted study with a BM-ADCP. Another possible explanation for this lower variance in cell 9 is side-lobe interference. If the side lobe of the acoustic signal is impinging on the bed, then the variance may be lower because of the contamination of the velocity data in cell 9 with data from a stationary object (the bed). However, it is important to note that no side-lobe interference has been confirmed for the H-ADCP at the time of this publication.

Rating Curves

The index velocity rating curves for the AVM and H-ADCP are linear in the velocity-velocity plane and do not appear to have a stage dependence. This relation is expected given the limited range of stage (approximately 573.7 to 580.6 ft above NAVD 88). Figures 18 and 19 show the rating curves for the AVM and H-ADCP, respectively. The index velocity ratings for the AVM and H-ADCP as determined by linear regression are

$$V_{mean} = 0.8914\, V_{AVM} - 0.0161 \quad (5)$$

$$V_{mean} = 0.8866\, V_{H-ADCP} + 0.0239 \quad (6)$$

where

V_{AVM} and $V_{H\text{-}ADCP}$ are the index velocities for the AVM and H-ADCP, respectively.

The coefficients of determination for the linear regressions are 0.9968 and 0.9955 for the AVM and H-ADCP ratings, respectively, and the standard error of the regression for the AVM is 0.045 compared to 0.051 for the H-ADCP. These regression statistics indicate both rating curves fit the observed data well, with a slightly better fit for the AVM rating. A total of 45 moving-boat ADCP discharge measurements collected between January 2005 and March 2010 were used to develop the AVM rating, whereas 42 measurements collected between June 2005 and March 2010 were used to define the H-ADCP rating.

For the 33 measurements that are common to both the AVM and H-ADCP ratings, the rated discharges computed with both ratings are very close to equal. Figure 20 shows the rated discharges plotted against one another with a line of equality shown for comparison. Over the full range of the measurements, the instruments compute very similar rated discharges with a slight deviation at very low discharges. At low flows, the H-ADCP computes a slightly higher rated discharge than the AVM. On the basis of the data presented above, this difference is likely owing to the complications in measurements resulting from secondary flows that occur at the site primarily under low-flow conditions.

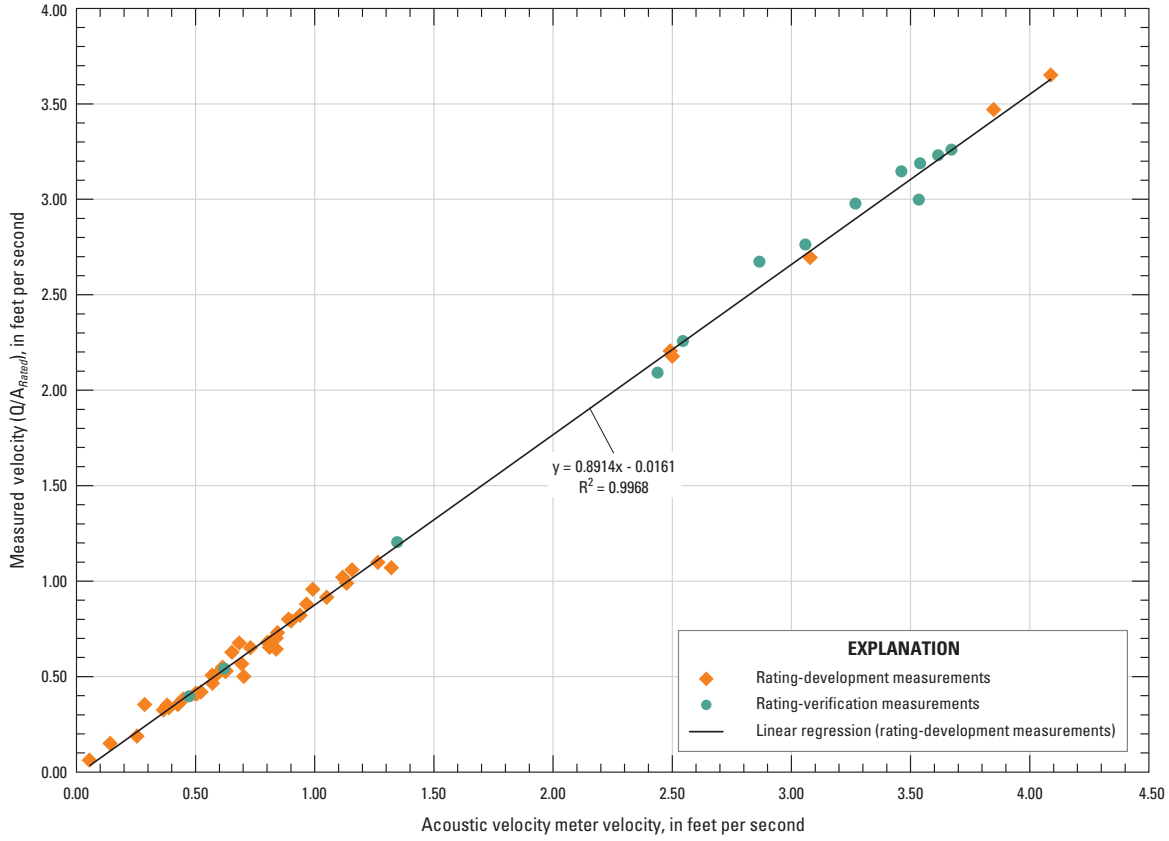

Figure 18. Index velocity rating curve for the acoustic velocity meter (AVM) deployed in the Chicago Sanitary and Ship Canal near Lemont, Illinois.

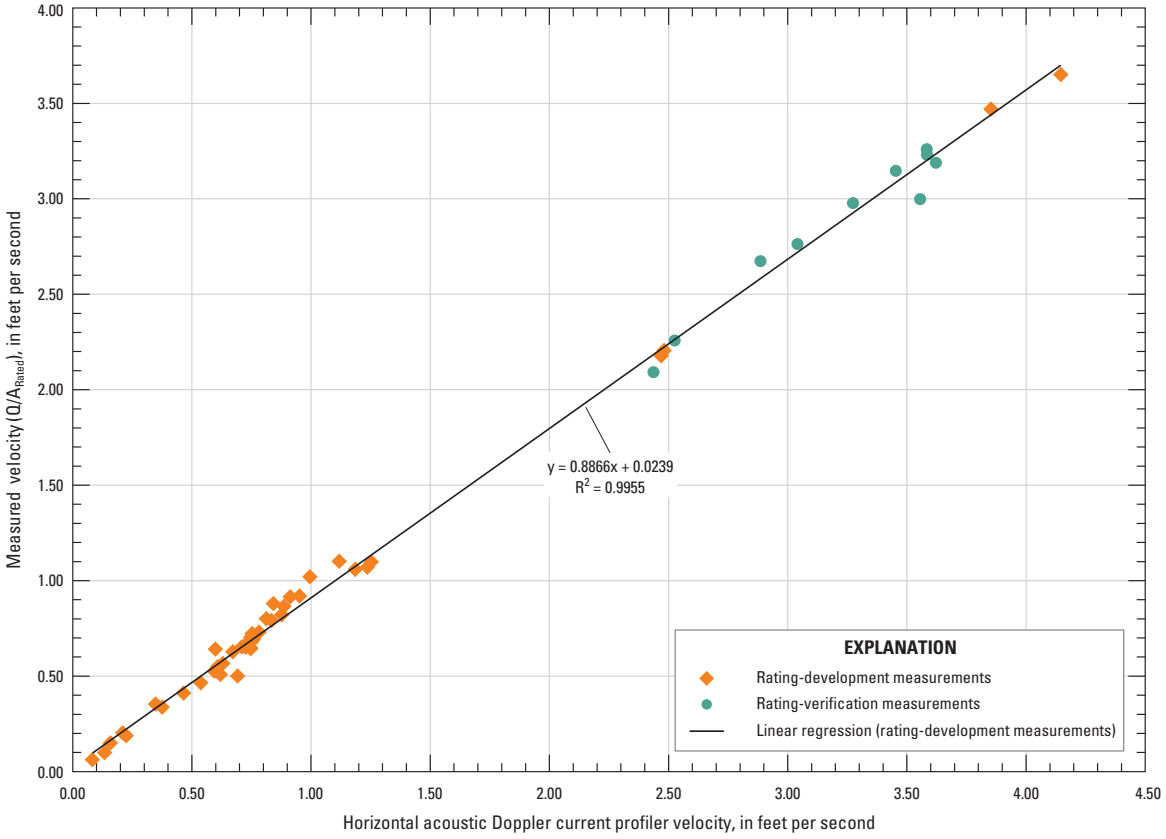

Figure 19. Index velocity rating curve for the horizontal acoustic Doppler current profiler (H-ADCP) deployed in the Chicago Sanitary and Ship Canal near Lemont, Illinois.

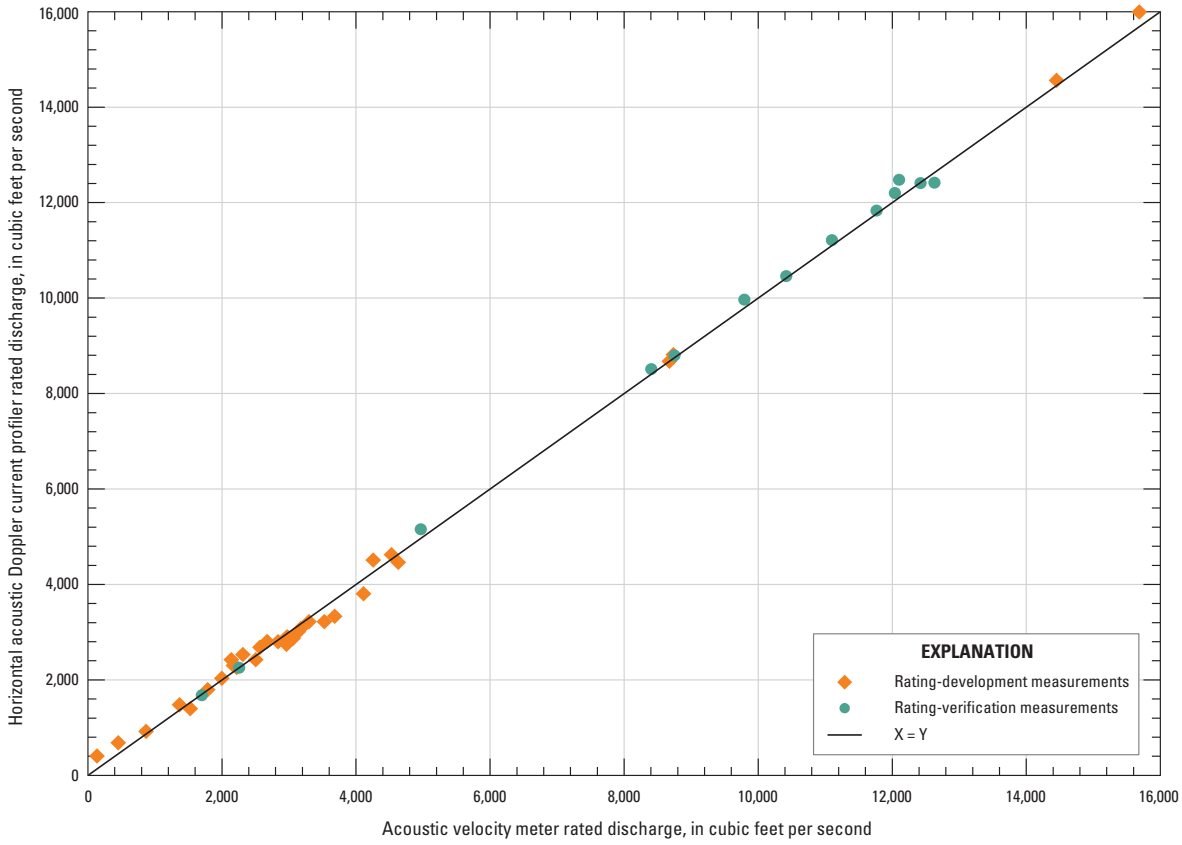

Figure 20. Comparison of rated discharges for the acoustic velocity meter (AVM) and horizontal acoustic Doppler current profiler (H-ADCP) for 33 discharge measurements in the Chicago Sanitary and Ship Canal near Lemont, Illinois.

Differences from the measured discharge are greatest at low flows and least at high flows for both instruments (fig. 21). At low flows (< 700 ft^3/s), the rated discharge for the H-ADCP is biased high and the rated discharge for the AVM is biased low. Low flows are inherently difficult to measure, owing to flow variability and instrument noise. On the basis of all the measurements used in the rating curve development, the AVM is biased high relative the measured discharge by 0.52 percent (median percent difference) and the H-ADCP is biased high by 1.43 percent (median percent difference). Overall, the AVM is the more accurate gage, with an overall median error of about one-third that of the H-ADCP based on 45 measurements for the AVM and 42 for the H-ADCP. In addition, the variance of the errors for the H-ADCP is 41 percent higher than the error variance for the AVM, indicating a greater variability in the rated H-ADCP discharge with respect to the true discharge. In general, for flows in the range 1,000 to 5,000 ft^3/s (the range most typical for the CSSC), most computed (instantaneous) discharges are within 10 percent of measured discharge. The percent errors in rated discharge for both instruments decrease with increasing discharge, and both instruments are within 2 percent of the measured discharge for flows greater than 8,000 ft^3/s. It is important to note that these percent differences are for short-duration discharge measurements, which are subject to instrument noise and flow variability. These errors are distributed about zero with median values that are less than 1.5 percent, and temporal averaging of the computed discharge at daily, monthly, and yearly timescales will reduce the error in the computed discharge. The next section compares computed discharge for both instruments at these timescales.

For comparison purposes, the uncertainty of mean annual discharge computed by means of the AVM and H-ADCP have been assessed by using the methodology of Duncker and others (2006). Assuming no uncertainty in BM-ADCP measurements, the estimated uncertainties in mean annual discharge are 0.91 percent and 1.6 percent for the AVM and H-ADCP, respectively. If one assumes a 1-percent uncertainty in both the rating-curve slope and intercept (an attempt at including the unknown uncertainty of BM-ADCP measurements), the estimated uncertainties in annual mean discharge are 3.3 percent and 4.4 percent for the AVM and H-ADCP, respectively.

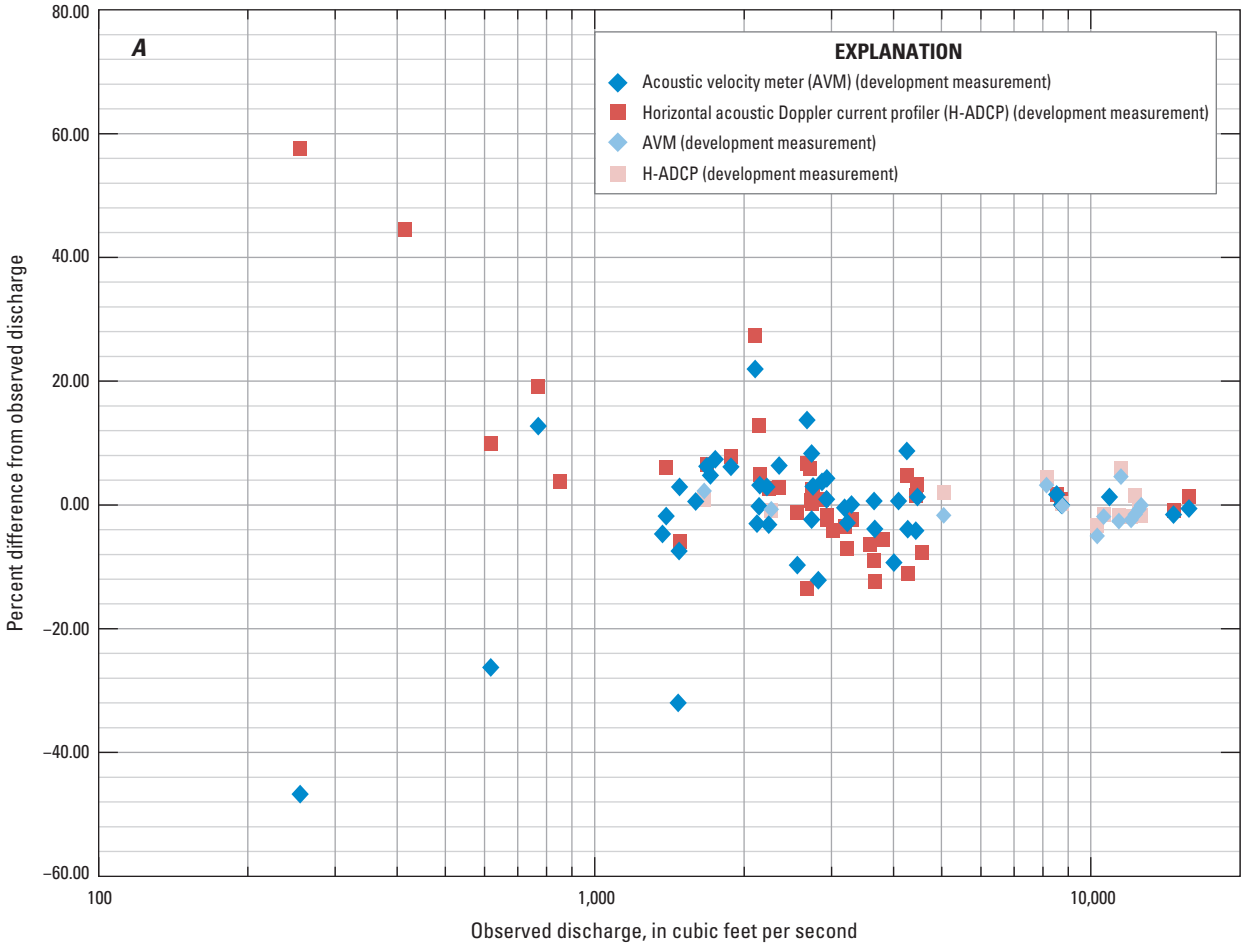

Figure 21*A*. Errors in rated discharge relative to the measured discharge for the acoustic velocity meter (AVM) and horizontal acoustic Doppler current profiler (H-ADCP) deployed in the Chicago Sanitary and Ship Canal near Lemont, Illinois.

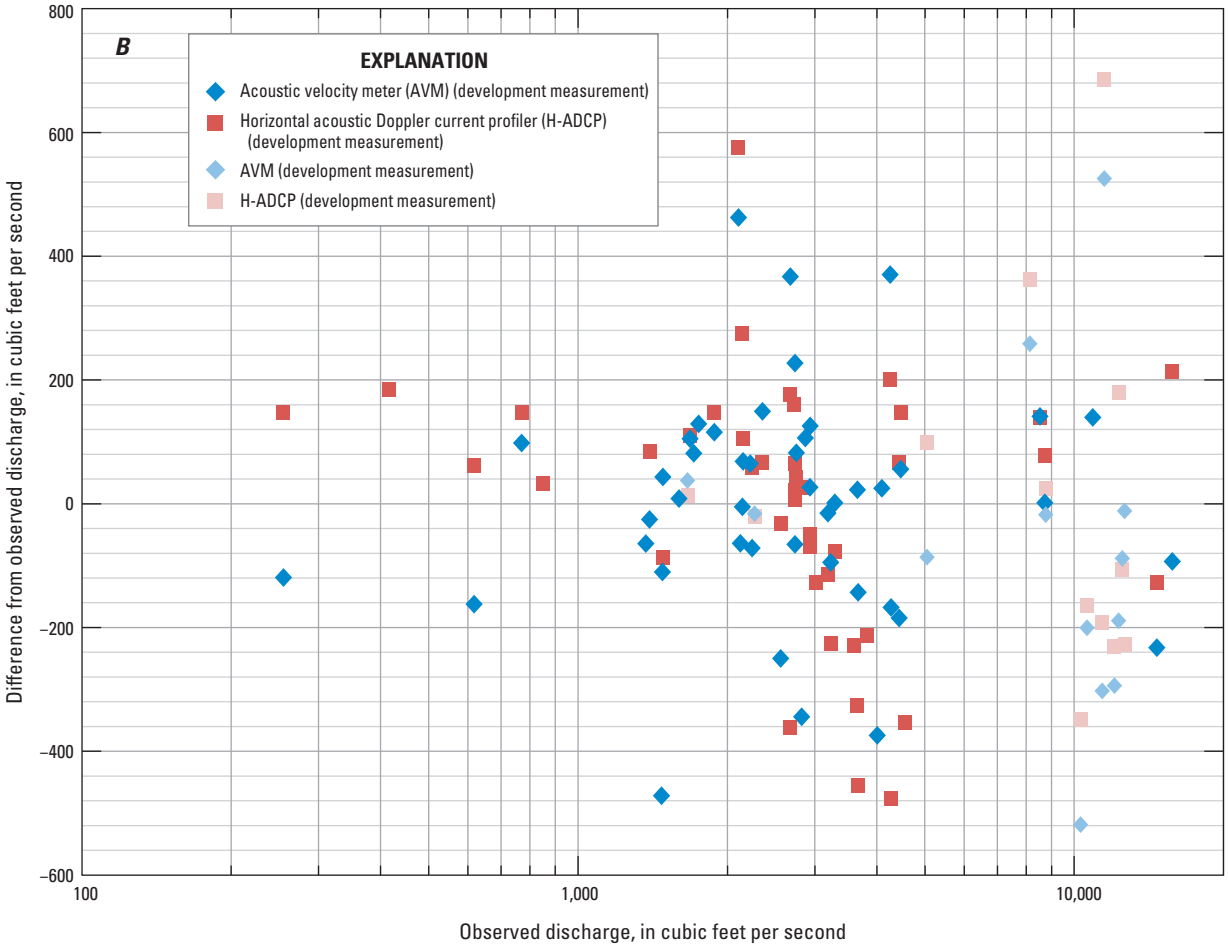

Figure 21*B*. Residuals in rated discharge relative to the measured discharge for the acoustic velocity meter (AVM) and horizontal acoustic Doppler current profiler (H-ADCP) deployed in the Chicago Sanitary and Ship Canal near Lemont, Illinois.

Computed Discharge

This section is dedicated to the comparison of computed discharge from the AVM and H-ADCP index velocity measurements in the CSSC near Lemont, Ill. Data used in this analysis include daily mean discharges for November 10, 2006, to December 31, 2010. From the computed discharge records for each instrument, days with estimated values or flagged data in either record have been removed from both records. This process ensures that only days in which both instruments were operational are being compared. In addition to comparing daily mean discharges, the following analysis also compares the monthly and annual mean discharges computed by using the index velocity method for the two instruments. It is important to understand that, for this analysis, annual mean values are for calendar years and not water years (October 1 to September 30) and that the annual mean for 2006 is a partial mean value (November 10, 2006, to December 31, 2006).

For the range of flows observed in the CSSC near Lemont, Ill., the AVM and H-ADCP mean daily, monthly, and annual computed discharges compare very well. Figure 22 is a scatterplot comparing the computed discharge data for both instruments at the three different time scales. For reference, a line of equal discharge also is plotted. The daily mean discharge data cloud lies along the line of equality with some scatter about the line. Above about 7,000 ft^3/s, the data plot primarily to the right of the line of equality, indicating that flows above 7,000 ft^3/s have a slightly lower computed discharge for the H-ADCP compared to the AVM. At flows above 14,000 ft^3/s, the data conform more closely to the line of equality. Both the monthly and annual mean discharges compare well between the AVM and H-ADCP and show considerably less variability both in range of observed discharge and deviation from the line of equality. The remainder of this section is dedicated to a more quantitative comparison of the discharge records by comparing the discharge distributions from each instrument and the difference between daily, monthly, and annual mean discharge for each instrument.

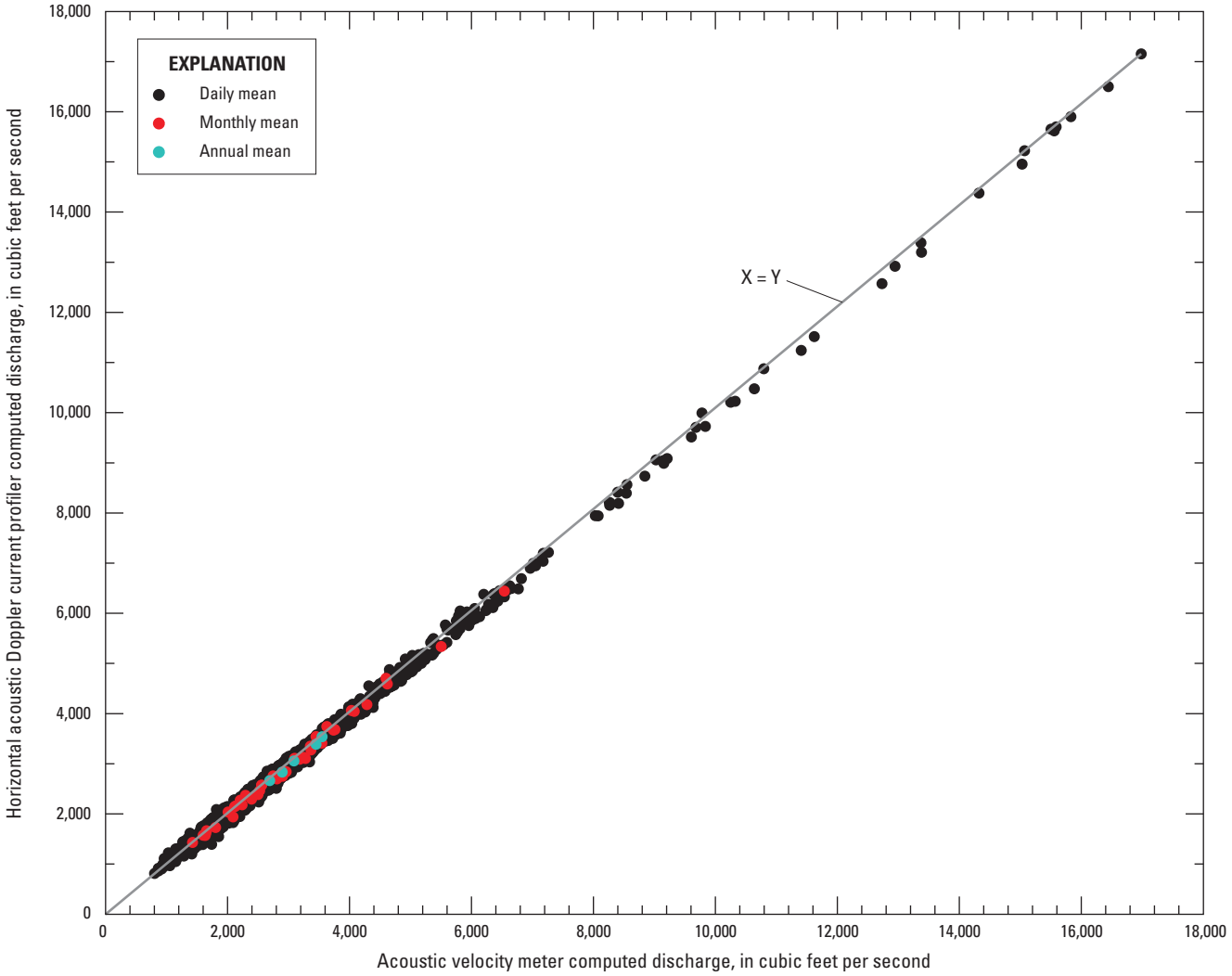

Figure 22. Scatterplot of the computed discharge (daily, monthly, and annual mean) for the acoustic velocity meter (AVM) and horizontal acoustic Doppler current profiler (H-ADCP) deployed in the Chicago Sanitary and Ship Canal near Lemont, Illinois, November 10, 2006, to December 31, 2010.

At a significance level of 5 percent, the distributions of daily, monthly, and annual mean discharges for the AVM and H-ADCP are not significantly different. At each time scale, the data distributions were compared by use of a two-sample Kolmogorov-Smirnov test and, in each case, the null hypothesis that the two samples come from the same continuous distribution was accepted at the 5-percent significant level. To further illustrate this equality in distributions, quantile-quantile plots are shown in figure 23 for each time scale. Data with equal distributions will fall along the $Y_{quantile} = X_{quantile}$ line. The data from the AVM and H-ADCP show no significant deviation from this line. The solid part of the line in each figure represents the region between the 25th and 75th percentiles. The distributions for both the daily and monthly mean discharges are highly skewed, whereas the distribution for annual mean discharge is symmetric (though only five data points are available for analysis).

Although differences between computed discharge for the AVM and H-ADCP are significantly different (in a statistical sense) for the daily mean values, differences at the monthly and annual time scales are not significantly different. Differences in computed discharge were computed for each pair of daily, monthly, and yearly mean values for the two instruments, plotted in boxplots (fig. 24), and compared by using a sign test. The sign test analyzes the differences and determines whether dataset 1 is generally larger (or smaller, or different) than dataset 2. At the 5-percent significance level, the test indicates that the computed daily mean discharges for the H-ADCP are lower than the AVM discharges (median difference of −59 ft^3/s). However, monthly and annual mean discharges computed for the H-ADCP are not statistically different from the AVM computed discharges when evaluated with the same sign test at the 5-percent significance level.

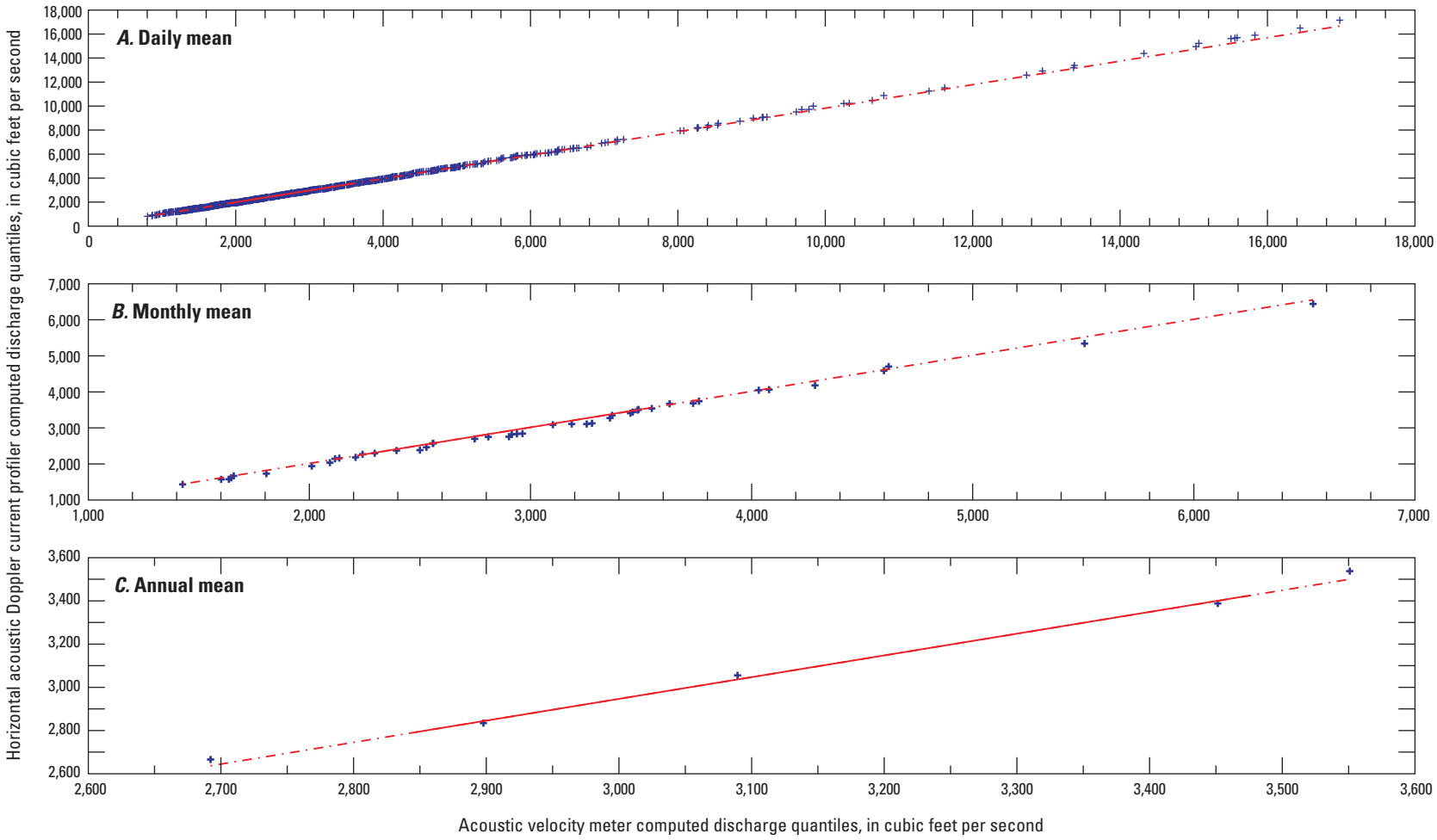

Figure 23. Quantile-quantile plots of mean daily, monthly, and annual computed discharges for the acoustic velocity meter (AVM) and horizontal acoustic Doppler current profiler (H-ADCP) deployed in the Chicago Sanitary and Ship Canal near Lemont, Illinois, November 10, 2006, to December 31, 2010.

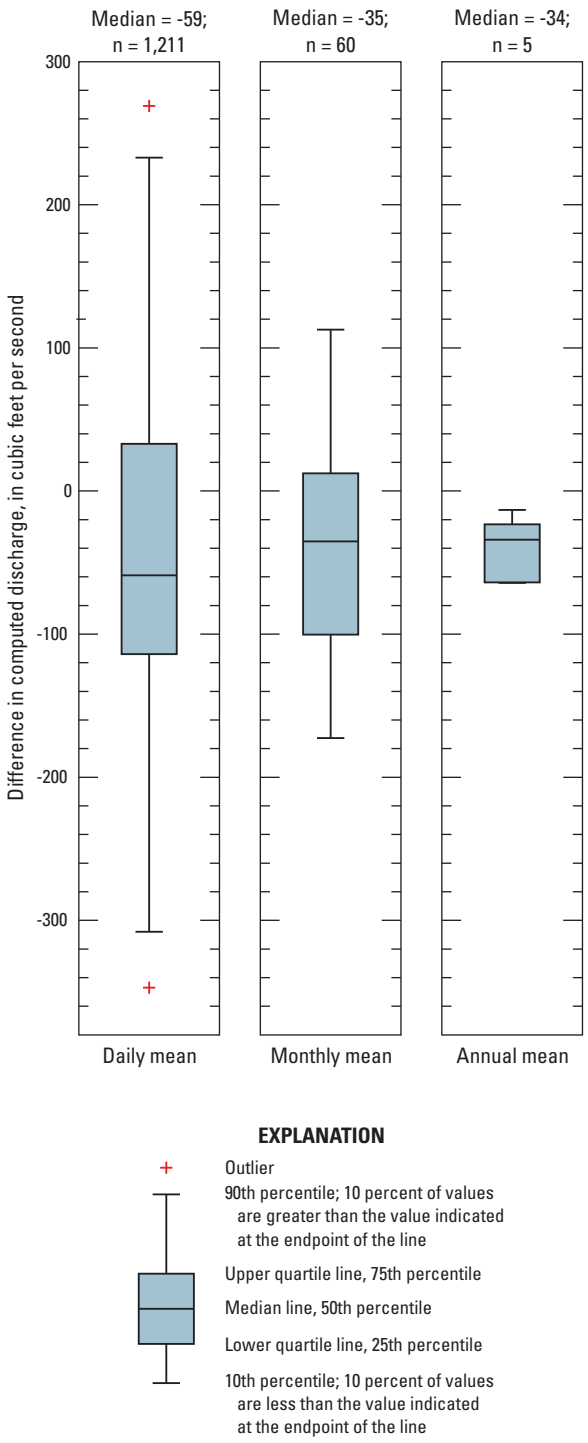

Figure 24. Boxplots of the difference in computed discharge (daily, monthly, and annual mean) for the acoustic velocity meter (AVM) and horizontal acoustic Doppler current profiler (H-ADCP) deployed in the Chicago Sanitary and Ship Canal near Lemont, Illinois, November 10, 2006, to December 31, 2010.

Therefore, in spite of having a median differences of −35 ft^3/s and −34 ft^3/s for the monthly and annual mean discharges, respectively, these differences could be attributed to chance and are not statistically significant according to the sign test at the 5-percent significance level. This finding indicates that temporal averaging of the data on a monthly and annual basis reduces the variability between the two datasets, thus making any differences statistically insignificant. Therefore, for the purposes of Lake Michigan diversion accounting in which the diversion is assessed on the basis of an annual mean discharge, the use of the H-ADCP-computed discharge in place of the AVM computed discharge is acceptable.

Conclusions

The State of Illinois' annual withdrawal from Lake Michigan is limited by a U.S. Supreme Court decree, and the U.S. Geological Survey is responsible for monitoring flows in the Chicago Sanitary and Ship Canal (CSSC) near Lemont, Ill., as a part of the Lake Michigan Diversion Accounting overseen by the U.S. Army Corps of Engineers, Chicago District. Every 5 years, a technical review committee consisting of practicing engineers and academics is convened to review the U.S. Geological Survey's streamgaging practices in the CSSC near Lemont, Ill. The sixth technical review committee raised a number of questions concerning the flows and streamgaging practices in the CSSC near Lemont, and this report provides answers to many of those questions. In addition, this report examines the index velocity meters in use at Lemont to determine whether the acoustic velocity meter (AVM), which is now the primary index velocity meter, can be replaced by the horizontal acoustic Doppler current profiler (H-ADCP), which is currently the backup meter. Although the AVM has performed well as the primary meter at Lemont, the unavailability of replacement parts and difficulty in making timely repairs have made it necessary to find a suitable replacement meter.

The flows in the CSSC near Lemont, Ill., cover a wide range of velocities and are highly unsteady. The primary source of unsteadiness appears to be the control of the Chicago Area Waterway System (CAWS) through three primary lock and dam structures. Control changes and lockages at the downstream end of the flow at Lockport, Ill., cause changes in the stage and flow elsewhere on the system, and the disturbances propagate through the system in the form of flood waves and seiches, both of which can be identified in the discharge records near Lemont. Withdrawals and discharges from powerplants and industry on the canal and wastewater inflows from three large water-reclamation plants further add variability to the flow. Storm-driven inflows from several tributaries on the Calumet Sag Channel and North Branch Chicago River and inflows from local runoff and combined-sewer overflows are yet other sources of flow variability, primarily during high flows. Localized and short-term flow variation near Lemont

is caused by commercial water traffic, which can be heavy in the Lemont area. A true understanding of the flow variability in the CSSC near Lemont requires one to unravel the complex time series that makes up the gage records at Lemont and trace each individual fluctuation in flow back to its source. Although this task is basically impossible, tools such as spectral analysis applied in this report can identify sources of flow variability that have a periodic component. Whereas large-scale seiches driven by control changes and lockages at Lockport appear to play a large role in the flow variability near Lemont, there is still much to be understood about flows in the CAWS. Understanding the role of each source of flow variability will require detailed hydrodynamic modeling in which each source of flow variability is represented accurately.

The success of an index-velocity-based discharge measurement depends on the flow characteristics at the site. If the velocity distribution in the measurement cross section is unique for every discharge (does not change for the same discharge), then one can theoretically develop an index velocity rating to compute discharge. In the CSSC near Lemont, the success of the index velocity method relies on the ability of the flow in the channel to conform to a set velocity distribution at every discharge and overcome local, transient flow disturbances. An examination of the vertical and transverse velocity profiles for a range of flows and temporal averaging periods revealed that although instantaneous flow profiles may be highly variable, temporally averaged profiles are generally consistent with open-channel flow theory. Therefore, temporal averaging is necessary near Lemont to average out the short-term variations in the flow owing to turbulence and the sources of flow variability discussed above. The length of the averaging interval is a tradeoff between the loss of resolution in the data caused by averaging true fluctuations in the discharge (which can occur over the course of a few minutes) and loss of accuracy in the index velocity rating caused by turbulence and other sources of flow variability causing local disruptions to the velocity distribution. Although an analysis of the averaging interval was not completed, the authors plan to complete such an analysis in the near future. Such an analysis would reveal whether the error in the rated discharge is dependent on sampling time and may help identify an averaging interval that minimizes this error. Finally, secondary flows were most prominent at low discharges and appeared to be partially responsible for large differences between the rated and measured discharge. Secondary flows have the ability to disrupt index velocity measurements because they introduce a flow angle, causing an erroneous index velocity to be computed. If the secondary flows were consistent at the site (that is, not varying in magnitude for a given discharge), they could be accounted for in the index velocity rating. Unfortunately, the secondary flows observed near Lemont appear to vary considerably at low flows and thus appear to be a source of error.

Use of bank-mounted instrumentation such as the AVM and H-ADCP appears to be the best option for index velocity measurement in the CSSC near Lemont. At this site, mounting instruments to the bed is very difficult, and up-looking ADCPs are placed on the channel bed and mounted on frames that do not have a fixed orientation. Therefore, up-looking ADCPs at this site rely on their compass and pitch and roll sensors to determine the correct orientation of the velocities measured above the unit. Commercial traffic caused significant disruptions to the compass readings on the deployed up-looking ADCPs, and a failure of the compass and pitch and roll sensors on an extended deployment corrupted a large dataset. Reliance on these sensors to determine an accurate and stable index velocity makes an up-looking ADCP less reliable than a bank-mounted H-ADCP (unless one installs the up-looking ADCP in a fixed, known orientation and uses the instrument coordinate system). The additional vulnerability of the instrument on the streambed to damage from commercial traffic and debris makes it less attractive than the H-ADCP for an AVM replacement.

Application of the AVM and H-ADCP to index mean channel velocity in the CSSC near Lemont, Ill., has produced good ratings to date. The site is well suited to index velocity measurements, and although the flows at the site display substantial primary and secondary flow variability, it is unlikely that one could find an alternative site between Romeoville and the Calumet Sag Channel confluence with the CSSC where these effects would not be present or would be lesser in magnitude. Location of the gage in this reach is essential to accurate accounting of the Lake Michigan Diversion. This reach is highly industrial and is a hub for commercial traffic on the CAWS. The current site of the gage is upstream of the main hub of commercial activity. Several aspects of the site add complexity to the analysis, including the sloughed right bank in the measurement reach and the proximity to the Calumet Sag Channel. The sloughed bank appears to be causing a flow acceleration through the measurement reach and may be responsible for influencing secondary circulation under certain flow conditions. The proximity to the confluence of the CSSC and Calumet Sag Channel may be responsible for flow deceleration near the left bank as observed in the H-ADCP data and moving-boat discharge measurements. Although both these factors have the ability to create changes in the flow structure and disrupt the index velocity rating, their overall effect on the ratings are small.

Comparison of the rating curves for the AVM and H-ADCP has revealed that the H-ADCP is a suitable replacement for the AVM as the primary index velocity meter near Lemont. Because of the smaller sampling volume and inherent uncertainty associated with Doppler measurements, the H-ADCP has slightly higher uncertainty than the AVM with regard to discharge computations. However, on the basis of velocity data collected during the past 4 years, the H-ADCP is more reliable than the AVM and is much less susceptible to disruptions from commercial traffic. Through a formal analysis of the effect of sampling time and averaging interval on measurement uncertainty near Lemont, it may be possible to further reduce the uncertainty in the H-ADCP. An added benefit of using the H-ADCP as the primary index velocity meter is the increased resolution of flow structure near Lemont. The

multicell design and two-dimensional velocity measurement capability of the instrument provides more information about the flow, making the H-ADCP an essential tool to understanding the influence of the Calumet Sag Channel on flows near Lemont.

The USGS gaging station on the CSSC near Lemont, Ill., is a key component to Lake Michigan Diversion Accounting . The importance of this station in monitoring withdrawals from Lake Michigan has made it one of the most highly scrutinized gaging stations in the country. Any changes in streamgaging practices at this gage requires detailed analysis to ensure the change will not adversely affect the ability of the USGS to accurately monitor flows. This report has provided a detailed analysis of the flow structure and index velocity measurements in the CSSC near Lemont, Ill., to ensure that decisions regarding the future of this gaging station are made with the best possible understanding of the site and the characteristics of the flow.

References Cited

Anderson, S., and Lohrmann, A., 1995, Open water test of the Sontek acoustic Doppler velocimeter, *in* Proceedings, IEEE Fifth Working Conference on Current Measurements, IEEE Oceanic Engineering Society, St. Petersburg, Fla.: p. 188–192.

Chen, Cheng-lung, 1991, Unified theory on power laws for flow resistance: Journal of Hydraulic Engineering, v. 117, no. 3, p. 371–389.

Dean, R.G., and Dalrymple, R.A., 1984, Water wave mechanics for engineers and scientists: Englewood Cliffs, N.J., Prentice-Hall, 353 p.

Duncker, J.J., Over, T.M., and Gonzalez, J.A., 2006, Computation and error analysis of discharge for the Lake Michigan Diversion Project in Illinois, 1997–99 water years: U.S. Geological Survey Scientific Investigations Report 2006–5018, 71 p.

Geyer, W.R., and Chant, Robert, 2006, The physical oceanography processes in the Hudson River Estuary, *in* Levinton, J.S., and Waldman, J.R., eds., The Hudson River Estuary: Cambridge, U.K., Cambridge University Press, p. 24–38.

González, J.A., Melching, C.S., and Oberg, K.A., 1996, Analysis of open-channel velocity measurements collected with an acoustic Doppler current profiler, *in* Proceedings of the First RIVERTECH International Conference, Chicago, Illinois, September 22–26, 1996: 8 p.

Jackson, P.R., García, C.M., Oberg, K.A., Johnson, K.K., and García, M.H., 2008, Density currents in the Chicago River—Characterization, effects on water quality, and potential sources: Science of the Total Environment, v. 401, p. 130–143.

Lane, S.N., Bradbrook, K.F., Richards, K.S., Biron, P.M., and Roy, A.G., 2000, Secondary circulation cells in river channel confluences—Measurement artefacts or coherent flow structures?: Hydrological Processes, v. 14, no. 11-12, p. 2047–2071.

Levesque, V.A., and Oberg, K.A., in press, Computing discharge using the index velocity method: U.S. Geological Survey Techniques and Methods 3-A23.

Morlock, S.E, Nguyen, H.T., and Ross, J.H., 2002, Feasibility of acoustic Doppler velocity meters for the production of discharge records from U.S. Geological Survey streamflow-gaging stations: U.S. Geological Survey Water-Resources Investigations Report 01–4157, 56 p.

Mueller, D.S., Abad, J.D., García, C.M., Gartner, J.W., García, M.H., and Oberg, K.A., 2007, Errors in acoustic Doppler profiler velocity measurements caused by flow disturbance: Journal of Hydraulic Engineering, v. 133, no. 12, p. 1411–1420.

Mueller, D.S., and Wagner, C.R., 2009, Measuring discharge with acoustic Doppler current profilers from a moving boat: U.S. Geological Survey Techniques and Methods 3A–22, 72 p. (Also available at *http://pubs.water.usgs.gov/tm3a22*.)

Ruhl, C.A., and Simpson, M.R., 2005, Computation of discharge using the index-velocity method in tidally affected areas: U.S. Geological Survey Scientific Investigations Report 2005–5004, 31 p.

Seo, I.W., and Baek, K.O., 2004, Estimation of the longitudinal dispersion coefficient using the velocity profile in natural streams: Journal of Hydraulic Engineering, v. 130, no. 3, p. 227–236.

U.S. Army Corps of Engineers, 1986, Illinois Waterway master reservoir regulation manual: Rock Island, Ill., Lockport Lock and O'Brien Lock and Controlling Works.